

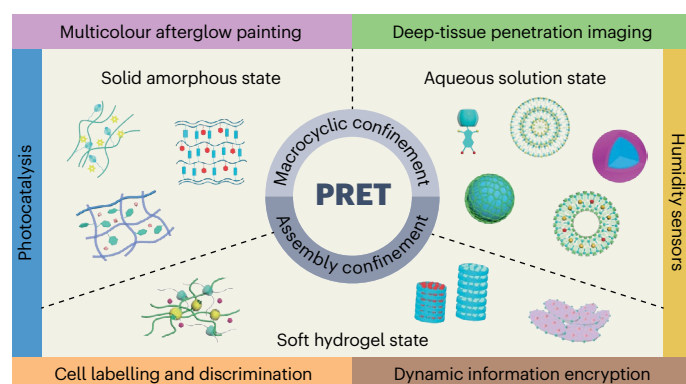
# Phosphorescence resonance energy transfer from purely organic supramolecular assembly

Xian-Yin Dai<sup>1,2</sup>, Man Huo<sup>1,2</sup> & Yu Liu<sup>1</sup>✉

## Abstract

Phosphorescence energy transfer systems have been applied in encryption, biomedical imaging and chemical sensing. These systems exhibit ultra-large Stokes shifts, high quantum yields and are colour-tuneable with long-wavelength afterglow fluorescence (particularly in the near-infrared) under ambient conditions. This review discusses triplet-to-singlet PRET or triplet-to-singlet-to-singlet cascaded PRET systems based on macrocyclic or assembly-confined purely organic phosphorescence introducing the critical roles of supramolecular noncovalent interactions in the process. These interactions promote intersystem crossing, restricting the motion of phosphors, minimizing non-radiative decay and organizing donor-acceptor pairs in close proximity. We discuss the applications of these systems and focus on the challenges ahead in facilitating their further development.

## Sections

[Introduction](#)[Solid supramolecular PRET systems](#)[PRET systems in aqueous solution](#)[PRET systems in hydrogels](#)[Concluding section](#)

<sup>1</sup>State Key Laboratory of Elemento-Organic Chemistry, College of Chemistry, Nankai University, Tianjin, P. R. China.

<sup>2</sup>These authors contributed equally: Xian-Yin Dai, Man Huo. ✉e-mail: [yuliu@nankai.edu.cn](mailto:yuliu@nankai.edu.cn)

## Introduction

Organic room-temperature phosphorescence (RTP) exhibits unique characteristics, including low toxicity, long emission lifetimes and large Stokes shifts<sup>1–5</sup>, which can be applied to many research fields, such as information technology<sup>6,7</sup>, biology<sup>8,9</sup> and materials science<sup>10–14</sup>. Numerous research activities have been devoted to the construction of RTP materials to reveal their photoluminescence behaviours and explore the applications. On the one hand, crystallization effectively induces RTP owing to the physical constraints, as well as multiple intermolecular interactions such as halogen bonding and hydrogen bonding<sup>15–20</sup>. On the other hand, polymerization<sup>21–23</sup>, incorporation into a rigid polymer matrix<sup>24–29</sup> and host–guest interactions<sup>30–36</sup> have also been recently devoted to the construction of RTP. However, achieving high quantum yields and a tunable afterglow emission, especially in the red or near-infrared (NIR) region under ambient conditions<sup>37–40</sup>, still remains an important challenge in organic phosphors owing to limits imposed by the energy-gap law<sup>41</sup>. Therefore, there is an urgent need to find alternative and versatile methods to achieve adjustable afterglow emission from purely organic chromophores. With the development of RTP, the phosphorescence resonance energy transfer (PRET) has received considerable attention, which addresses the above issues via the triplet-to-singlet energy transfer process<sup>42–47</sup>.

Singlet-to-singlet Förster resonance energy transfer (SS-FRET) is allowed between singlet states in which the spin angular momentum is conserved over the long-distance (1–10 nm) dipole–dipole interactions<sup>48–51</sup>. Dexter energy transfer, represented by triplet–triplet energy transfer (TTET), is another spin-allowed photophysical process within limited short-range distances (<10 Å), which directly exchanges electrons between molecules or intramolecular fragments as electron shells overlap or donor and acceptor parts come into contact<sup>52,53</sup>. These principles of TTET can be used to construct high-efficiency phosphorescent materials in addition to resonance energy transfer mechanisms<sup>54,55</sup>. Compared with SS-FRET and TTET, the triplet-to-singlet FRET (TS-FRET, also referred to as phosphorescence resonance energy transfer, PRET) is defined as the process when energy is transferred from an excited triplet state (phosphorescence donor) to an excited singlet state (fluorescence acceptor). This occurs according to the inductive–resonant mechanism without conserving the spin angular momentum when increasing spin–orbital coupling interactions of the triplet and singlet excited states<sup>56–59</sup>. Specifically, an electron-excited singlet donor generates an electron-excited singlet acceptor in an SS-FRET process, such as  $^1D^* + ^1A \rightarrow ^1D + ^1A^*$ , whereas PRET yields a long-lived singlet species from a triplet excited donor:  $^3D^* + ^1A \rightarrow ^1D + ^1A^*$ . Similarly, a triplet species is produced from a triplet excited donor during TTET:  $^3D^* + ^1A \rightarrow ^1D + ^3A^*$ .

The following key factors typically need to be taken into consideration when designing a new PRET system: (1) the strong oscillator strength of the phosphorescence donor emission (strong spin–orbit coupling and intense phosphorescence intensity), (2) the coincident donor emission with acceptor absorption, (3) a suitable physical donor–acceptor distance (1–10 nm) and (4) the approximately parallel orientation of the responsible transition dipole moments. The PRET process guarantees that after a suitable organic fluorescent dye with good spectral overlap as an energy acceptor is introduced, the energy can be transferred from an excited triplet state of the donor to an excited singlet state of the acceptor, ultimately yielding red-shifted long-lived delayed fluorescence emission in macrocyclic or assembly-confined conditions<sup>60,61</sup>. Moreover, colour-tunable afterglow fluorescence, especially long-lived NIR emission, can be readily

achieved by using different fluorescent dyes, which greatly circumvents the tedious molecular design and synthesis process<sup>62–65</sup>.

Generally, the design strategies for purely organic phosphorescence donors include the incorporation of lone-pair electrons (heteroatoms or aromatic carbonyl groups) into functional groups according to El-Sayed's rule – which undergo an orbital-type change when spin multiplicity changes – and the introduction of non-metallic heavy atoms (chlorine, bromine, iodine and so on) to strengthen spin–orbit coupling and RTP intensity<sup>66,67</sup>. The acceptors should also be highly fluorescent dyes, possessing small Stokes shift to minimize spectral energy loss in the triplet-to-singlet PRET process besides matching spectrally and being at suitable distances from phosphorescence donors<sup>68,69</sup>. Therefore, the first step in constructing such supramolecular PRET systems is to achieve high-performance RTP with high quantum yields and long phosphorescence lifetimes, ensuring that the triplet-to-singlet transitions can acquire appreciable oscillator strength under strong spin–orbit coupling. Not only does this make the transition quantum-mechanically feasible, but it also facilitates the non-radiative dipole–dipole interactions and consequent energy transfer from the triplet excited state of the donor to the ground state of the acceptor<sup>70–73</sup>. Moreover, phosphorescence donors present efficient spin–orbit coupling, thus having two potential FRET donor states; the singlet-to-singlet energy transfer and triplet-to-singlet energy transfer would simultaneously occur if the fluorescence spectrum of the donor matches the absorption spectrum of the acceptor<sup>74,75</sup>. However, the Dexter energy transfer between donor–acceptor triplets may happen if a fluorescent acceptor is used as a dopant in a pure phosphorescent donor with a proximity of less than 1 nm and overlapping molecular orbitals. Such doping results in the effective loss of excitons when they reach the acceptor triplet state owing to the extremely inefficient phosphorescence effect of fluorescent acceptor dyes<sup>76</sup>. In this context, macrocyclic or assembly-confined small-molecule phosphorescence donors can prevent their aggregation and ensure that the donor–acceptor distance exceed 1 nm; thus, the part played by Dexter energy transfer is negligible.

Supramolecular assembly derived by the cooperative contributions of diverse noncovalent interactions, such as electrostatic, hydrophobic, ion–dipole, hydrogen bonding and host–guest interactions, provides an attractive strategy for constructing PRET systems<sup>77–79</sup>. These assemblies immobilize phosphors' motion, suppressing the non-radiative decay to obtain high-efficiency RTP emission, while concurrently creating a confined environment for subsequent delayed sensitization process offering an available platform for the development of PRET systems<sup>80–85</sup>. Typically, macrocycles such as cucurbit[*n*]urils (*n* = 7 or 8),  $\alpha$ -/ $\beta$ -cyclodextrins ( $\alpha$ -/ $\beta$ -CD) and amphiphilic lower-rim aliphatic-modified sulfonatocalix[4]arenes (SC4A[*n*], *n* = 4, 6 or 12) and functional polymers such as polyvinyl alcohol (PVA), polyacrylamide (PAA), polymethyl methacrylate (PMMA), polyvinyl pyrrolidone (PVP), modified hyaluronic acid (HA), triblock copolymer poly(ethylene glycol)-block-poly(propylene glycol)-block-poly(ethylene glycol) (PEG-b-PPG-b-PEG, also named F127) and Laponite clay (LP) are able to encapsulate or co-assemble with guest compounds or host–guest complexes to enhance phosphorescence and undergo energy transfer process after introducing suitable fluorescent acceptors (Fig. 1). In this Review, we discuss the development of the one-step triplet-to-singlet PRET and stepwise triplet-to-singlet-to-singlet cascaded PRET from macrocyclic or assembly-confined purely organic phosphorescence. Specifically, we discuss these PRET systems in the solid amorphous state, aqueous

solution state and hydrogel state; we also discuss their potential applications in dynamic information encryption, colourful afterglow painting, deep-tissue penetration imaging, cell labelling and discrimination, photochemical catalysis, and reversible humidity sensors. Finally, we offer our perspectives on the current challenges and potential future directions of purely organic supramolecular assemblies of PRET, providing a guide for the design and construction of more advanced PRET systems with excellent properties to promote cross-fertilization and rapid development of related disciplines.

### Solid supramolecular PRET systems

For constructing solid supramolecular PRET systems, the first thing to consider is to create efficient RTP emission by promoting intersystem crossing and preventing the non-radiative relaxation through the confinement effect, as well as minimizing oxygen quenching of the excited triplet excitons<sup>86</sup>. The next step is to select energy level-matched acceptor chromophores, while organizing and confining the donor and acceptor chromophores appropriately to minimize the donor–acceptor distance and align the dipole–dipole orientations between the excited donor and ground-state acceptor<sup>87</sup>. A series of ingenious approaches have been developed such as using phosphorescent donors or acceptors as dopants in rigid polymeric films through covalent or noncovalent strategies or grafting phosphorescent functional groups onto the polymer by copolymerization with acrylamide. These methods effectively suppress non-radiative deactivation and reorient doped molecules through weak secondary interactions, such as hydrogen bonding and interaction between donor, acceptor and the solid matrices, to achieve efficient colourful afterglow emission in co-assembled confinements with a variety of applications in painting, humidity sensing and information encryption.

### Polymer-mediated solid-state supramolecular assemblies

Water-soluble PVA contains multiple pendant hydroxyl functional groups which can assemble directly with phosphors through noncovalent interactions such as ion–dipole or hydrogen bonding interactions to form PVA-based solid-state supramolecular structures<sup>88–90</sup> (Fig. 2a). A series of purely organic PRET systems with long phosphorescence lifetimes and high phosphorescence quantum yields have been derived from this strategy. For example, water-soluble coronene tetracarboxylate salt (CS) incorporated into the rigid PVA polymer matrix acts as a triplet energy donor aided by ion–dipole and hydrogen bonding interactions between the carboxylates of CS and the hydroxyl groups of PVA, presenting greenish-yellow afterglow at 532 nm with ultralong phosphorescence lifetimes ( $\tau$ ) of 2.46 s and excellent RTP quantum yield of 23.4% in air<sup>91</sup> (Fig. 2b). Further doping appropriate fluorescent acceptor molecules whose absorption overlaps well with the RTP emission – such as commercially available Sulpharhodamine G (SRG,  $\lambda_{em} = 560$  nm) and Sulpharhodamine 101 (SR101,  $\lambda_{em} = 610$  nm) – produces long, persistent, narrow-bandwidth and colour-tunable delayed fluorescence of the otherwise short-lived singlet states of the acceptor chromophores through the delayed sensitization process. This is also accompanied with a good triplet-to-singlet energy transfer efficiency ( $\Phi_{ET} > 65\%$ ) for both fluorescent molecules. The sulphonates and sulphonic acid groups in SRG and SR101 ensure the secondary interactions between the acceptor chromophores and the PVA matrix, facilitating an efficient co-assembly and maintains a close donor–acceptor distance, which results in an efficient energy transfer process. In addition, this CS-SRG-PVA or CS-SR101-PVA assemblies can be prepared on a large-scale and exhibit high air stability while

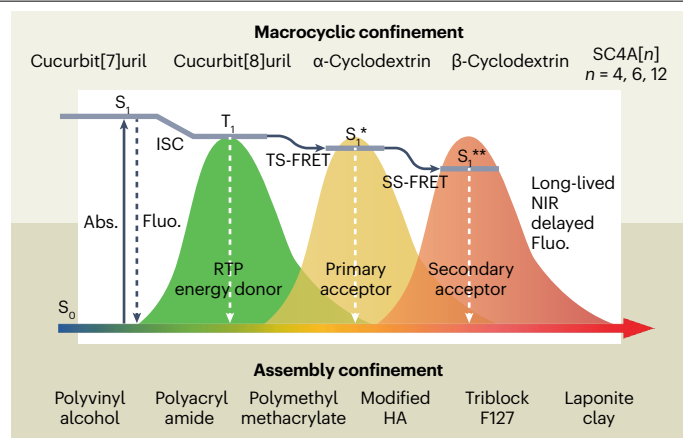


**Fig. 1 | Simplified Jablonski diagram illustrating the PRET or cascaded PRET process owing to macrocylic confinement and assembly confinement.** The macrocylic confinement is based on various macrocycles including cucurbit[7]uril, cucurbit[8]uril,  $\alpha$ -cyclodextrin,  $\beta$ -cyclodextrin and sulfonatocalix[4]arenes (SC4A[n],  $n = 4, 6, 12$ ), whereas the assembly confinement relies on different functional polymers such as polyvinyl alcohol, polyacrylamide, polymethyl methacrylate, modified hyaluronic acid (HA), triblock copolymer poly(ethylene glycol)-block-poly(propylene glycol)-block-poly(ethylene glycol) (F127) and Laponite clay. The green, yellow and red colours represent the emission spectra of room-temperature phosphorescence (RTP) donors, primary acceptors and secondary acceptors, respectively. Abs., absorption; Fluo., fluorescence; FRET, Förster resonance energy transfer; ISC, intersystem crossing; NIR, near-infrared;  $S_0$ , ground state of donor;  $S_1$ , lowest singlet state of donor;  $S_1^*$ , lowest singlet state of primary acceptor;  $S_1^{**}$ , lowest singlet state of secondary acceptor; SS, singlet-to-singlet;  $T_1$ , lowest triplet state of donor; TS, triplet-to-singlet.

being self-standing, flexible and water processable, providing ideas for fabricating PVA-based PRET systems in the future.

Moreover, introducing dual-interaction sites into phosphors through molecular engineering that can interact specifically with PVA to increase their electrostatic attraction can also be used to lead to the construction of organic ultralong PRET systems. For example, the four indolocarbazole isomers, 5,11-ICz, 5,7-ICz, 5,12-ICz and 11,12-ICz<sup>92</sup> (Fig. 2c), contain two N–H bonds each, adopt planar conformations and can be simply embedded into the PVA matrix to generate a rigid co-assembly with excellent RTP property ( $\lambda_{em} = 461$  nm, 495 nm, 465 nm and 460 nm, respectively) including ultralong lifetimes from 0.38 s to 2.04 s and high phosphorescence quantum yields from 5.5% to 44.1%. The syn-isomer, 11,12-ICz, preferred to form two hydrogen bonds with a single PVA chain – opposed to hydrogen bonding with different chains – favouring the stabilization of triplet-state emission and was conducive to forming rigid co-assemblies within the PVA matrix, thus leading to the most efficient blue-colour RTP afterglows. Furthermore, such indolocarbazole isomer-doped PVA systems can be adopted as energy donors to achieve persistently colour-tunable delayed fluorescence afterglows ranging from green to red by adjusting the type of organic fluorescent acceptor dye – such as sodium fluorescein (Fluo,  $\lambda_{em} = 534$  nm), Rhodamine 6G (Rh6G,  $\lambda_{em} = 574$  nm) and Rhodamine B (RhB,  $\lambda_{em} = 596$  nm). These experiments established the structure–property relationship based on the similarity of the indolocarbazole isomers and revealed the impact on RTP properties owing to the hydrogen bonding interactions with the PVA matrix, and also offered new

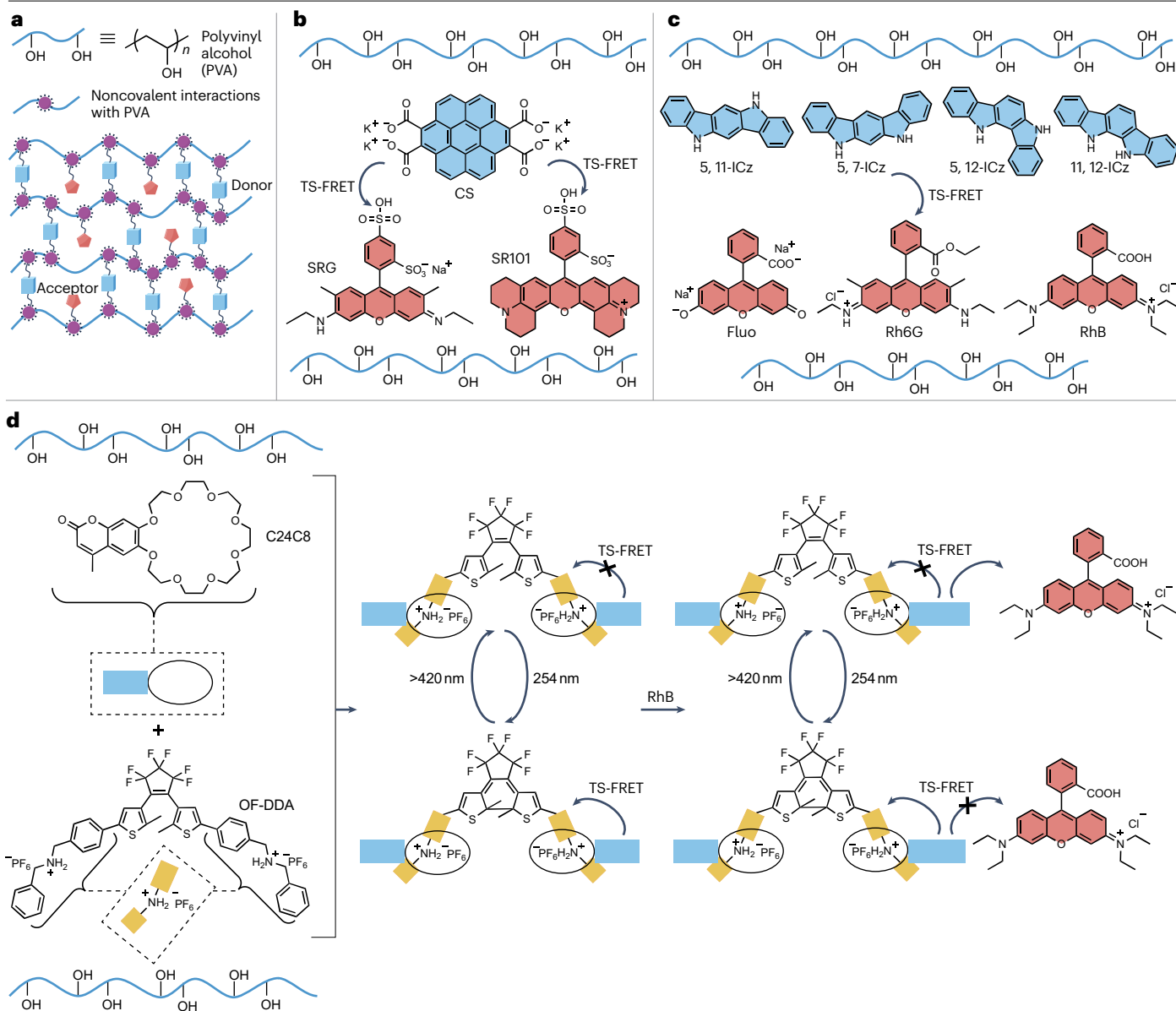


**Fig. 2 | Polyvinyl alcohol (PVA)-mediated solid-state supramolecular assemblies for PRET by direct doping.** **a**, Schematic representation of how to fabricate solid PRET systems by directly doping phosphorescence donors (blue rectangles) and fluorescence acceptors (red pentagons) into a PVA matrix. **b**, Ambient afterglow fluorescence at 560 or 610 nm based on the co-assembly of coronene tetracarboxylate salt (CS) and fluorescence acceptors Sulpharhodamine G (SRG) or Sulpharhodamine 101 (SR101) in PVA, respectively. **c**, Organic long persistent luminescence based on the co-assembly

of indolocarbazole (ICz) isomers and fluorescence acceptors such as fluorescein (Fluo), Rhodamine 6G (Rh6G) and Rhodamine B (RhB) in PVA ( $\lambda_{em} = 534, 574$  and  $596$  nm, respectively). **d**, Phosphorescence energy transfer photo-switch based on the co-assembly of coumarin-24-crown-8 (C24C8), diarylethene dicationic alkylammonium (OF-DDA) and RhB with PVA. TS-FRET is not allowed from C24C8 to the open form OF-DDA in the absence of RhB (indicated by X marks), whereas triplet-to-singlet Förster resonance energy transfer (TS-FRET) from the C24C8 to RhB is allowed in the presence of RhB under the same conditions.

guidelines for constructing afterglow materials. Nitrogen-containing heterocyclic 5-amino-1,10-phenanthroline also exhibited RTP when co-assembled with a PVA matrix, which gave a phosphorescence lifetime of up to 229.4 ms and photoluminescence quantum yield (PLQY) of 19.6%, and PRET process occurred when Rh6G or RhB was doped into the PVA co-assemblies yielding afterglow colour ranging from green and yellow to orange<sup>93</sup>. Pyridine-substituted triphenylamine

derivatives in PVA matrices have also presented ultralong RTP, in which the pyridine groups reduced the energy gap to enhance intersystem crossing (ISC) efficiency, and formed hydrogen bonding interactions with the matrix to stabilize triplet excitons whereafter multicolour organic afterglows were obtained through PRET<sup>94</sup>. Interestingly, some aromatic macrocycle crown ethers also exhibit considerable RTP emission through crystallization or co-assembly with PVA matrices<sup>95</sup>.

Coumarin-24-crown-8 (C24C8, Fig. 2d) emitted green afterglow RTP at 516 nm with a lifetime of 528.03 ms after assembling with PVA. Its ring binds tightly with the diarylethene dicationic alkylammonium derivatives through hydrogen bonding of N–H···O and C–H···O to achieve a photo-switchable RTP afterglow with good reversibility under alternating ultraviolet (UV) and visible light irradiation. This switch can function as the donor for TS-FRET with RhB acceptor ( $\Phi_{ET} = 88.3\%$ ), in which a highly efficient RTP energy transfer process from C24C8 to RhB can be remotely dominated<sup>96</sup>. The photo-switched phosphorescence material can be used in time-resolved information encryption and lays the foundation for constructing afterglow PRET photo-switches via host–guest interaction.

Furthermore, the pendant hydroxyl groups in PVA chains can form covalent B–O bond linkages between polymer matrices and boronic acid group-functionalized phosphors through simple dehydration condensation reactions under alkaline conditions, which activates highly efficient RTP emission<sup>97,98</sup>. The compound 1,1':3',1''-terphenyl-5'-boronic acid (DPP-BOH) can react with PVA chains to emit blue RTP at 475 nm with a corresponding lifetime of up to 2.43 s and phosphorescence quantum yield reaching 7.51%<sup>99</sup> (Fig. 3Aa). The molecular tightness of DPP-BOH can be controlled more effectively through the covalent B–O bond than through hydrogen bonding interactions (Fig. 3Ab). Moreover, benefiting from good spectral overlap (Fig. 3Ac), DPP-BOH-PVA systems could serve as the energy donor and co-assemble with an energy acceptor such as Fluo or RhB to obtain Fluo-DPP-BOH-PVA or RhB-DPP-BOH-PVA, respectively, with tunable afterglow colours from blue to green or orange and lifetimes of 1.60 s at 533 nm ( $\Phi_{ET} = 13.85\%$ ) and 1.90 s at 581 nm ( $\Phi_{ET} = 9.47\%$ ) (Fig. 3Ad–f), respectively. The calculated oscillator strength of the phosphorescence donor DPP-BOH-PVA was large enough (0.0078) which could facilitate the dipole–dipole coupling with Fluo or RhB. Furthermore, a humid environment would destroy the intra-chain or inter-chain hydrogen bonding interactions of the PVA matrix – originally stiff owing to its inherent hygroscopicity – in which the PRET process and afterglow phenomena could be reversibly controlled by the alternating humidity and temperature (Fig. 3Ag). Examples of this humidity responsiveness are the environmentally friendly phosphorescence inks with water-processable properties which have shown great practical application in screen printing, secondary anti-counterfeiting and fingerprint record collection.

Compared with one-step triplet-to-singlet PRET, stepwise triplet-to-singlet-to-singlet cascaded PRET can also be used to construct longer-wavelength persistent luminescence, particularly long-lived NIR emission. Typically, the triphenylene-2-ylboronic acid (TP) was embedded into a PVA matrix yielding a persistent blue phosphorescence system with an ultralong lifetime of 3.29 s and high phosphorescence quantum yield of 33.1% in air<sup>100</sup> (Fig. 3Ba). The introduction of boronic acid groups into triphenylene greatly enhances ISC efficiency and triplet exciton population in TP granting the strong phosphorescence. TP-PVA can first be co-assembled with an intermediate red dye acceptor RhB ( $\lambda_{em} = 590$  nm) or Nile red (NiR,  $\lambda_{em} = 650$  nm) to form RhB-TP-PVA or NiR-TP-PVA, and then further co-assembled with a final NIR dye Cyanine 7 (Cy7,  $\lambda_{em} = 808$  nm) to obtain Cy7-RhB-TP-PVA or Cy7-NiR-TP-PVA. Taking Cy7-RhB-TP-PVA as an example, with increasing amounts of RhB up to 10 mol%, the original lifetime at 470 nm gradually decreased from 3.29 to 1.78 s (Fig. 3Bc), and the delayed RhB emission showed the highest persistent luminescent intensity at 590 nm with an ultralong lifetime of 0.86 s (Fig. 3Bb,d). Moreover, a stepwise FRET process occurred as indicated by the emerging NIR peak

at 820 nm when the RhB-TP-PVA system was doped with up to 10 mol% Cy7 (Fig. 3Be), in which the lifetime at 470 nm was further reduced to 0.90 s (Fig. 3Bf) and the lifetime at 590 nm of RhB decreased to 0.58 s (Fig. 3Bg). This ultimately achieved persistent NIR luminescence up to 0.16 s for Cy7-RhB-TP-PVA and was successfully applied in penetrating NIR bioimaging<sup>100</sup> (Fig. 3Bg).

Whereas PVA has a considerable confinement effect towards water-soluble phosphors when preparing solid supramolecular PRET systems, most water-insoluble phosphorescence donors are more inclined to co-assemble with organic phase polymer matrix, such as PMMA, semi-crystalline syndiotactic polystyrene (sPS) and PVP, to create amorphous purely organic PRET systems. Efficient singlet-to-singlet FRET and triplet-to-singlet PRET occurred simultaneously from both singlet and triplet states of one single photoluminescent molecule when *N,N'*-di(naphtha-1-yl)-*N,N'*-diphenylbenzidine and 4-(dicyanomethylene)-2-*tert*-butyl-6-(1,1,7,7-tetramethyljulolidyl-9-enyl)-4*H*-pyran were implanted into the rigid PMMA polymer matrix as donor and acceptor, respectively (Fig. 4A). This system inhibited the depopulation of non-radiative triplet excitons and avoided the aggregation of small organic molecules, which promoted the singlet-to-singlet and triplet-to-singlet energy transfer<sup>101</sup>. However, if molecules have high-efficiency ISC and strong RTP emission with weak fluorescence contribution, as well as the RTP emission possessing an invalid spectral overlap integral with the acceptor absorption, singlet-to-singlet FRET does not tend to occur. A conjugate of dibenzofuran phosphor and dithienylbenzothiophene photo-switch formed a two-in-one photoluminescent molecule named o-BFT, which exhibited dual emission of fluorescence ( $\lambda_{em} = 445$  nm) and RTP ( $\lambda_{em} = 530$  nm) in vacuum when present as a dopant in sPS polymer films owing to the molecular configuration locking, and reduced the non-radiative dissipation of excited triplet excitons<sup>102</sup> (Fig. 4Ba). Intriguingly, o-BFT-sPS still achieved reversible absorption changes before and after UV irradiation (Fig. 4Bc). In addition, the green afterglow of o-BFT-sPS could be reversibly quenched and recovered through a light-controllable intermolecular triplet-to-singlet energy transfer process based on the light-activated photocyclization and decyclization of o-BFT when exposed to alternate UV and visible light irradiation (Fig. 4Bb,d). Moreover, the average lifetime of the o-BFT-sPS film at 530 nm reduced drastically from 22.3 ms to 141.2  $\mu$ s upon continuous irradiation at 365 nm in vacuum (Fig. 4Be). The absent singlet–singlet FRET preserved its inherent fluorescence emission and obtained a photo-reversible fluorescence–RTP switch – a convenient approach for photo-manipulation of singlet–triplet luminescence behaviours. For polymer confinement effects, PVP as a rigid matrix can not only avoid the quenching effect caused by phosphor 6-chlorothiochroman-4-one (CTO) self-aggregation but also suppress its non-radiative transition and shield its triplet state from oxygen quenching, achieving efficient cyan phosphorescence emission at 470 nm<sup>103</sup> (Fig. 4C). Incorporating an acceptor such as 4,4'-(hexane-1,6-diyl)bis(3*H*-1,2,4-triazole-3,5(4*H*)-dione) (HTD,  $\lambda_{em} = 570$  nm) with visible light-decomposing features into the phosphorescent CTO-PVP system led to low phosphorescence intensity owing to TS-FRET. However, the phosphorescence signal gradually recovered because of a photodegradation process of HTD caused by visible light. The design strategy of introducing molecules with photo-degradation characteristics as acceptors broadened the range of stimulus-responsive materials based on the PRET process. Likewise, PMMA-based RTP materials doped with a series of heteroatom-free or heavy atom-free polycyclic aromatic hydrocarbons, such as truxene ( $\lambda_{em} = 480$  nm) and coronene ( $\lambda_{em} = 565$  nm), showed the

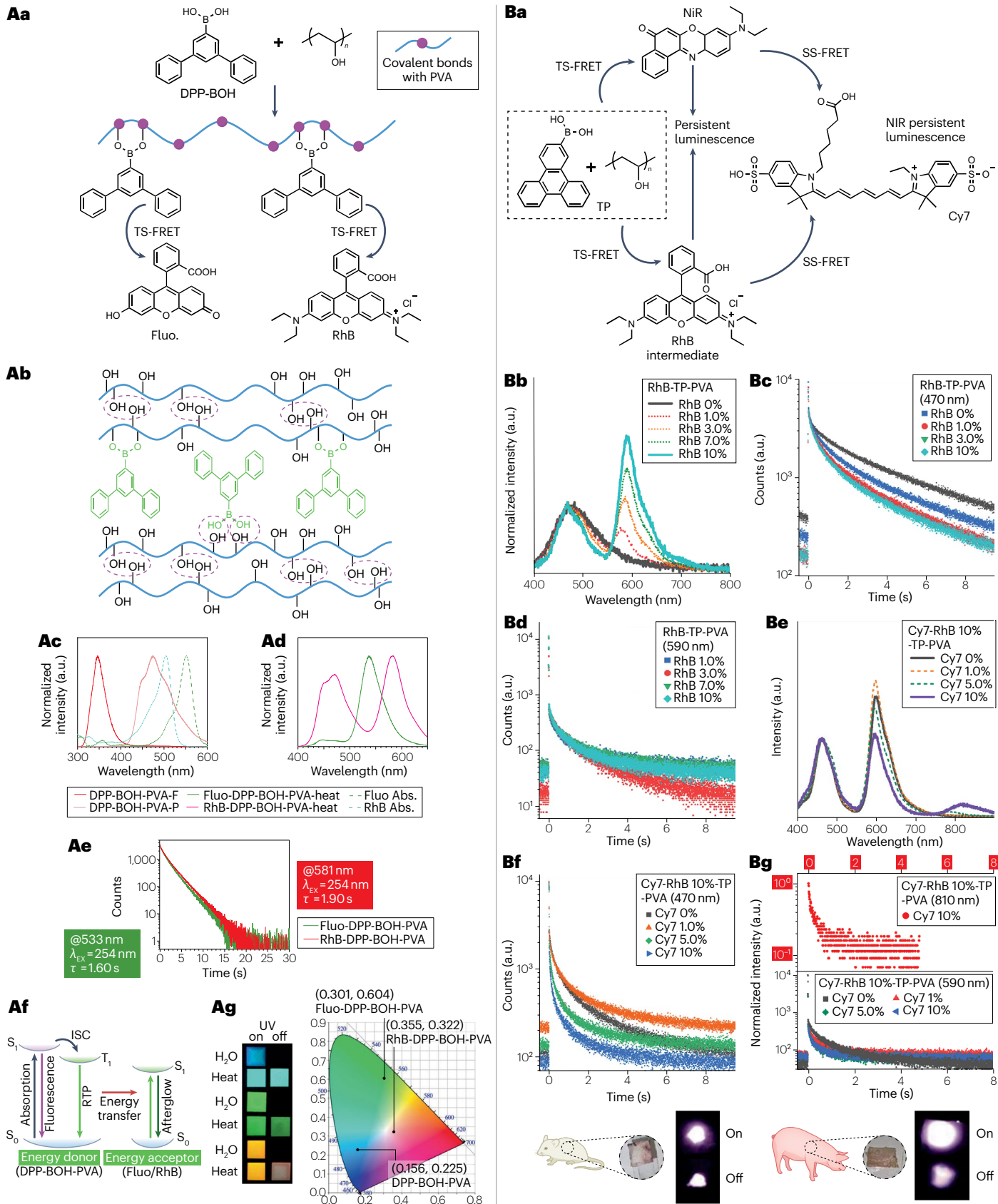


**Fig. 3 | Polyvinyl alcohol (PVA)-mediated solid-state supramolecular assemblies for PRET through covalent B–O bonds.** **Aa**, Stimulus-responsive afterglows by introducing fluorescein (Fluo) or Rhodamine B (RhB) into the matrix in which B–O covalent bonds form between 1,1':3',1''-terphenyl-5'-boronic acid (DPP-BOH) and polyvinyl alcohol (PVA). **Ab**, Dashed lines around the OH groups refer to hydrogen bonding interactions between PVA chains. **Ac**, Fluorescence spectra of DPP-BOH-PVA (DPP-BOH-PVA-F,  $\lambda_{em} = 345$  nm), room-temperature phosphorescence (RTP) spectra of DPP-BOH-PVA (DPP-BOH-PVA-P,  $\lambda_{em} = 475$  nm) and UV–vis absorption spectra of Fluo and RhB. **Ad, e**, Normalized RTP spectra and lifetimes of Fluo-DPP-BOH-PVA and RhB-DPP-BOH-PVA at 533 and 581 nm, respectively. **Af**, Simplified Jablonski diagram illustrating the PRET process ( $S_0$ ,  $S_1$  and  $T_1$  refer to ground, lowest singlet

and lowest triplet state, respectively; ISC, intersystem crossing). **Ag**, Photos of DPP-BOH-PVA, Fluo-DPP-BOH-PVA and RhB-DPP-BOH-PVA before and after heating and Commission Internationale de l'Éclairage (CIE) coordinates of the afterglows. **Ba**, Near-infrared (NIR) persistent luminescence based on stepwise energy transfer from triphenylene-2-ylboronic acid (TP), to intermediate dyes, Nile red (NiR) or RhB, and finally to a NIR dye Cyanine 7 (Cy7). **Bb–d**, Delayed spectra of RhB-TP-PVA with varied RhB concentrations, and their lifetimes at 470 and 590 nm. **Be–g**, Delayed spectra of Cy7-RhB-TP-PVA with varied Cy7 concentrations, and their lifetimes at 470, 590 and 810 nm. Photos of Cy7-RhB-TP-PVA emission were taken through a piece of mouse or pork skin. Part **A** was adapted from ref. 99 under a Creative Commons licence CC BY 4.0. Part **B** was adapted with permission from ref. 100, Wiley.

degree of conjugation-dependant afterglows from blue to green with a lifetime of >5 s at ambient conditions<sup>104</sup> (Fig. 4D). Further co-doping with a fluorescent dye, perylene red, can red-shift the wavelength of afterglow up to 650 nm with a lifetime of 2.8 s from the PRET process, which ultimately achieved the full-colour afterglows and demonstrated excellent results in information storage, dynamic anti-counterfeiting and oxygen sensing. The pure hydrocarbons with the weak spin–orbit coupling can also produce long-lived phosphorescence owing to a slow radiative ISC transition from first excited triplet state to the singlet ground state. Besides, the triphenyl phosphonium containing polymer acceptors can be doped into the PMMA matrix with different triphenylamine derivative donors to create photo-induced long-lived phosphorescence emission at ambient conditions, benefiting from the donor–acceptor interactions and the molecular oxygen consumption features of PMMA<sup>105</sup>.

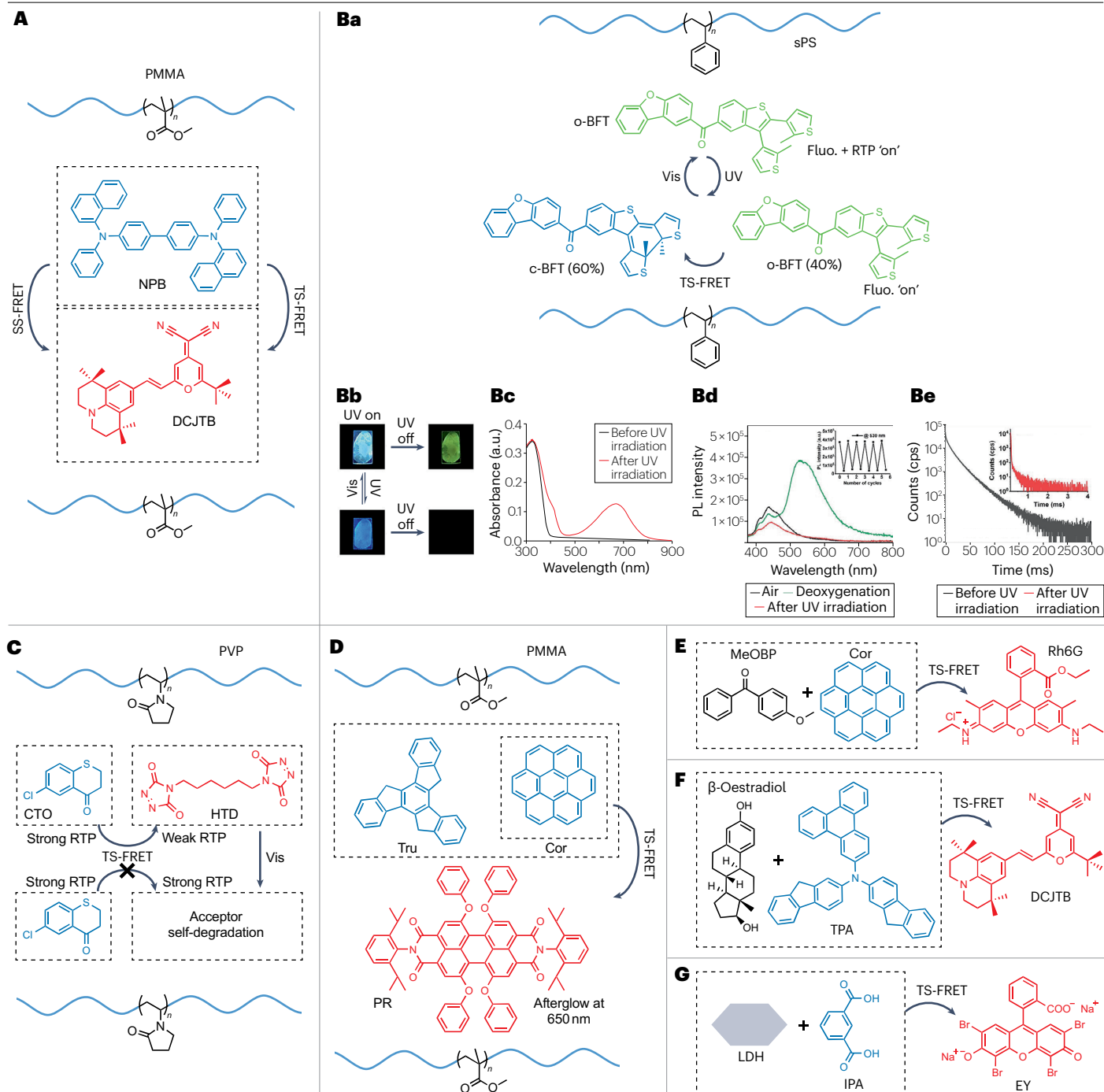
In solid supramolecular PRET systems, 4-methoxybenzophenone (MeOBP)<sup>106</sup> (Fig. 4E), hydroxyl steroidal compounds ( $\beta$ -oestradiol)<sup>107</sup> (Fig. 4F) and layered double hydroxide<sup>108</sup> (Fig. 4G) can also be used as rigid host matrices to stabilize the excited triplet state through the confinement effect and protect phosphors' triplets from oxygen quenching, ensuring the strength of the oscillator and RTP intensity for effective PRET, thus resulting in efficient persistent afterglows.

### Copolymerization-constructed solid-state supramolecular assemblies

Different from doping polymer matrices with phosphor, the copolymer-assembly confinement by grafting phosphorescent molecules into the polymer in situ forms a dense hydrogen-bonded network of amino and carbonyl groups. These networks can inhibit the non-radiative relaxation of phosphorescent molecules by the rich presence of hydrogen bonding interactions leading to highly efficient RTP emission<sup>109,110</sup>. Specifically, the covalent integration of phosphors into the PAA chains via copolymerization can substantially prompt singlet-to-triplet intersystem crossing and inhibit non-radiative deactivation of phosphors, and simultaneously create a microenvironment to isolate phosphorescence quenchers. For example, water-soluble amorphous poly(acrylamide-co-*N*-vinylcarbazole) (PAACz) prepared through a binary radical copolymerization of acrylamide and vinyl carbazole<sup>111</sup> (Fig. 5A) showed blue afterglow emission along with ultralong RTP lifetime of 4.2 s. In light of the large spectral overlap between the phosphorescence spectrum and absorption spectra of fluorescent guests such as sodium 3,9-perylene dicarboxylate ( $\lambda_{em} = 502$  nm), sodium fluorescein ( $\lambda_{em} = 560$  nm), Rhodamine 123 (Rh123,  $\lambda_{em} = 575$  nm) and Rhodamine B ( $\lambda_{em} = 618$  nm), as well as effective dipole–dipole coupling, full-colour organic afterglow including blue, green, yellow and red was,

respectively, obtained by phosphorescence sensitization strategy after doping into the above blue polymeric matrix. Particularly, white afterglow could also be acquired by regulating the doping weight concentration of Rh123. These full-colour afterglow polymers with water-soluble characteristics can act as environmentally friendly printing inks for time-resolved multicolour security printing. This study offered an insightful guideline on producing full-colour afterglow materials with on-demand modulation. Additionally, the current organic afterglow materials always suffered from insufficient colour purity (broad emission peak) and low photoluminescence quantum efficiency. Functional copolymer, polyacrylamide quinolino-3,2,1-deacidine-5,9-dione (PAAQA), emits bright-green emission ( $\lambda_{em} = 504$  nm) with high PLQY of 88.9% and high-efficiency hyperafterglow at half-maximum of 38 nm by covalently anchoring multi-resonance, thermally activating delayed fluorescence chromophores with acrylamide<sup>112</sup>. Further combination with afterglow host PAACz (PAACzQA) can prolong the lifetime of this hyperafterglow emission to 1.64 s based on the efficient energy transfer. Strikingly, the pure-green hyperafterglow emission of PAACzQA can be further modulated to pure red ( $\lambda_{em} = 636$  nm) with a lifetime of 1.16 s by using a red narrowband emitter as guest, which were used in hyperafterglow light-emitting diode and display panels and revealed a new design method for constructing hyperafterglow materials based on PRET process.

In order to extend the RTP performance of copolymerization-constructed solid-state supramolecular assemblies, macrocyclic hosts are introduced to interact with the phosphorescence units on the polymer leading to synergistic confinement phosphorescence emission. A series of host–guest RTP systems with controllable phosphorescence lifetime ranging from 0.9 s to 2.2 s were successfully constructed by virtue of the intense host–guest interactions between macrocyclic cucurbit[7]uril (CB[7]) and 4-phenylpyridium derivatives-grafted acrylamide polymers (P-R)<sup>113</sup> (Fig. 5B). CB[7] can effectively improve the original RTP performance of P-R owing to the further macrocyclic confinement effect. Organic dyes such as Eosin Y (EY) ( $\lambda_{em} = 568$  nm) or SR101 ( $\lambda_{em} = 620$  nm) have great UV–vis absorption overlap with RTP emissions of CB[7]-phosphorescent copolymers (Fig. 5Da), and they can serve as energy acceptors in highly efficient PRET processes with long-persistent polychrome delayed fluorescence. P-CN/CB[7]-SR101 exhibits two delayed emissions located at 504 nm and 620 nm, respectively (Fig. 5Db), the latter of these emissions (620 nm) is consistent with the fluorescence emission of SR101 in PAA also located at 620 nm, confirming the delayed fluorescence nature (Fig. 5Dc). It can also be applicable to afterglow paints and encryption, and granted an effective approach for developing various ultralong-lifetime RTP materials and high-performance multicolour persistent luminescence materials.



Moreover, the simultaneous covalent embedding of a purely organic phosphor donor and energy acceptor into the matrix of a polymer via ternary radical copolymerization is another tactful strategy to generate effective phosphorescent emission and perform PRET. To this end, a series of amorphous acrylamide copolymers were prepared by copolymerizing an energy phosphorescent donor di(but-3-en-1-yl) terephthalate (DT,  $\lambda_{em} = 425$  nm) and acceptor dimethyl 2,5-bis((2-(pent-4-enoyloxy)ethyl)amino)terephthalate (DEAT,  $\lambda_{em} = 580$  nm) with a single benzene and precise spectral overlap. This copolymer

(P-DT-DEAT) displayed a tunable afterglow emission, especially ambient white emission with a quantum yield of 27.2% by adjusting the different ratios through the TS-FRET<sup>14</sup> (Fig. 5E). Notably, this donor-acceptor copolymerization strategy can be effective in improving the energy transfer efficiency owing to the shorter molecular distance between donor and acceptor from the copolymerization process. Such simple-structured single-benzene-based copolymers provided a new perspective on the design and construction of ambient afterglow materials.

**Fig. 4 | Alternate rigid polymer matrix-mediated solid-state supramolecular assemblies for PRET.** **A**, Simultaneous singlet–singlet and triplet–singlet emission from *N,N'*-di(naphtha-1-yl)-*N,N'*-diphenylbenzidine (NPB) and 4-(dicyanomethylene)-2-*tert*-butyl-6-(1,1,7,7-tetramethyljulolidyl-9-enyl)-4*H*-pyran (DCJTB) in polymethyl methacrylate (PMMA). **Ba**, Photo-reversible fluorescence–RTP switching with ultraviolet (UV) and visible light based on a conjugate of dibenzofuran phosphor and dithienylbenzothiophene photo-switch (o-BFT) and semi-crystalline syndiotactic polystyrene (sPS) in vacuum. **Bb,c**, Fluorescence and afterglow photos of o-BFT-sPS before and after 365 nm irradiation in vacuum, and their UV–vis absorption spectra. **Bd**, Photoluminescence spectra of o-BFT-sPS in air and vacuum, after UV irradiation in vacuum, and their phosphorescence intensity ( $\lambda_{em} = 530$  nm) switching. **Be**, Lifetimes of o-BFT-sPS in vacuum before and after UV irradiation. **C**, Photoactivated organic RTP based on the

6-chlorothiochroman-4-one (CTO) and 4,4'-(hexane-1,6-diyl)bis(3*H*-1,2,4-triazole-3,5(4*H*)-dione) (HTD) in polyvinyl pyrrolidone (PVP) ( $\lambda_{em} = 570$  nm). ('X' indicates that TS-FRET is not allowed.) **D**, Full-colour ultralong afterglows based on heteroatom-free hydrocarbons such as truxene (Tru, blue afterglow,  $\lambda_{em} = 480$  nm) or coronene (Cor, green afterglow,  $\lambda_{em} = 565$  nm) and perylene red (PR, red afterglow,  $\lambda_{em} = 650$  nm) in PMMA. **E**, Small-molecule 4-methoxybenzophenone (MeOBP)-mediated solid PRET system based on Cor and Rh6G. **F**, Amorphous  $\beta$ -oestradiol-mediated solid PRET system based on triphenylamine derivative (TPA) with an amino-conjugated substituent. **G**, Layered double hydroxide (LDH)-mediated solid PRET system based on isophthalic acid (IPA) and Eosin Y (EY). Part **B** adapted with permission from ref. 102, Wiley. Flu., fluorescence; FRET, Förster resonance energy transfer; LP, Laponite clay; PRET, phosphorescence resonance energy transfer; RTP, room-temperature phosphorescence; TS-FRET, triplet-to-singlet FRET.

Consequently, by implanting functional moieties with photochromic properties as energy acceptors into acrylamide phosphorescent copolymers, the occurrence of PRET can be achieved by remote photo-control, thus realizing non-invasive dynamic reversible modulation of the emission behaviour of supramolecular phosphorescent materials. Based on photochromic spiropyran (SP,  $\lambda_{em} = 625$  nm), benzaldehyde (BA,  $\lambda_{em} = 510$  nm) and 2,5-dihydroxy terephthalate (DhT,  $\lambda_{em} = 520$  nm), three polyacrylamide polymers have been designed by copolymerizing BA and SP (P-BA-SP), DhT and SP (P-DhT-SP), and BA, DhT and SP (P-BA-DhT-SP), respectively, in which the blue-green phosphorescence gradually declined and turned to orange-pink under 365 nm irradiation owing to PRET from phosphorescent donors to the fluorescent merocyanine state of SP<sup>115</sup> (Fig. 5C). Long-lived multicolour conversions with favourable reversibility and fatigue resistance related to photoluminescence intensity were achieved upon the alternating exposure of 365 nm UV and visible light irradiation and explored for light-printing or light-erasing to decrypt or encrypt information. Besides, the unique feature of SP responsive to temperature also endowed the multicolour emissions of SP which involved these three polymers at various temperatures. These systems showing tunable multicolour emissions by integrating red, green and blue pave the way to acquire smart displayed materials via a non-invasive photo-controlled manner. Additionally, the fabrication of light-responsive purely organic RTP-assembled systems with ultrahigh emission quantum yields has been fraught with challenges. Similarly, copolymerized 4-(6-bromonaphthalenyl)pyridine derivatives with acrylamide as a new supramolecular building block can construct solid-state supramolecular tunable, ultra-strong white light-emitting system with PLQY of 83.9% quantum yield<sup>116</sup> (Fig. 5F). Distinct from the classical host–guest encapsulation with cyclodextrins, the negatively multi-charged sulfobutylether- $\beta$ -cyclodextrin electrostatically interacted with positively charged 4-(6-bromonaphthalenyl)pyridine copolymer, thereby further improving the phosphorescent quantum yield from 64.1% to 71.3% owing to the assembly-confined effect. Next, the photochromic nonfluorescent diarylethene derivatives as copolymer units were attached to the mentioned binary supramolecular system, and the reversible phosphorescence emission was achieved by efficient light-controlled PRET with the phosphorescence quenching efficiency reaching 55.3%. Using the excellent photo-switchable luminescence behaviour and multicolour tunable properties of the system, the supramolecular system was successfully created for applications in white light-emitting diodes, stimuli-responsive phosphorescent inks and information encryption.

This work provided an inspiring design strategy for high-efficiency purely organic phosphorescent materials at ambient conditions and with unprecedentedly high quantum yields.

As demonstrated in Supplementary Tables 1 and 2, PVA confinement and acrylamide copolymerization played a major part in PRET for polymer-mediated solid-state supramolecular assemblies and copolymerization-constructed solid-state supramolecular assemblies, respectively. The rich hydrogen bonding interactions inside the doped polymer systems and acrylamide copolymer systems help to stabilize the molecular conformation and protect phosphors from quenchers to obtain high-efficiency RTP with ultralong seconds-level lifetimes. They also guarantee the effective colour-tunable and red-shifted afterglow outputs, especially NIR emission, via the PRET process in such confinements. In view of the excellent solution processability and ambient stability of these solid-state afterglow assemblies, the applications in multicolour dynamic information encryption with printing technology and anti-counterfeiting technology were developed, which provided important guidance on exploring high-performance afterglow materials for further optoelectronic applications.

### PRET systems in aqueous solution

Unlike the solid phosphorescence supramolecules for PRET, the triplet excitons in aqueous media are more susceptible to quenching by water molecules and dissolved oxygen<sup>117,118</sup>. Thus, the phosphors should be isolated from water and molecular oxygen<sup>119</sup>, and at the same time, the donor–acceptor groups should keep an ordered spatial organization (suitable orientation, close distance within 10 nm) to reduce the potential energy losses<sup>120,121</sup>. At present, PRET systems operating in aqueous solution are formed by co-assembling phosphors with macrocyclic compounds such as CB[n] ( $n = 7, 8$ ),  $\alpha$ -/ $\beta$ -CDs and amphiphilic molecules such as SC4A[n] ( $n = 4, 6$  or 12) and triblock copolymer F127, which rendered synergistic hydrophobic shielding and confined rigidification effects, as well as loading fluorescent dyes to conduct PRET process, possessing great application potential in biomedical imaging.

### Amphiphilic macrocyclic cascaded assemblies

Amphiphilic macrocycles are used as assembly units to perform cascaded assembly to overcome triplet excitons being quenched by water molecules and dissolved oxygen in aqueous solution<sup>122</sup>. The cascaded assembly strategy was proposed to prevent quenching based on the synergistic electrostatic and hydrophobic interactions between CB[n]-mediated host–guest complexes and amphiphilic macrocyclic compounds (Fig. 6A). This strategy restricted the motion of

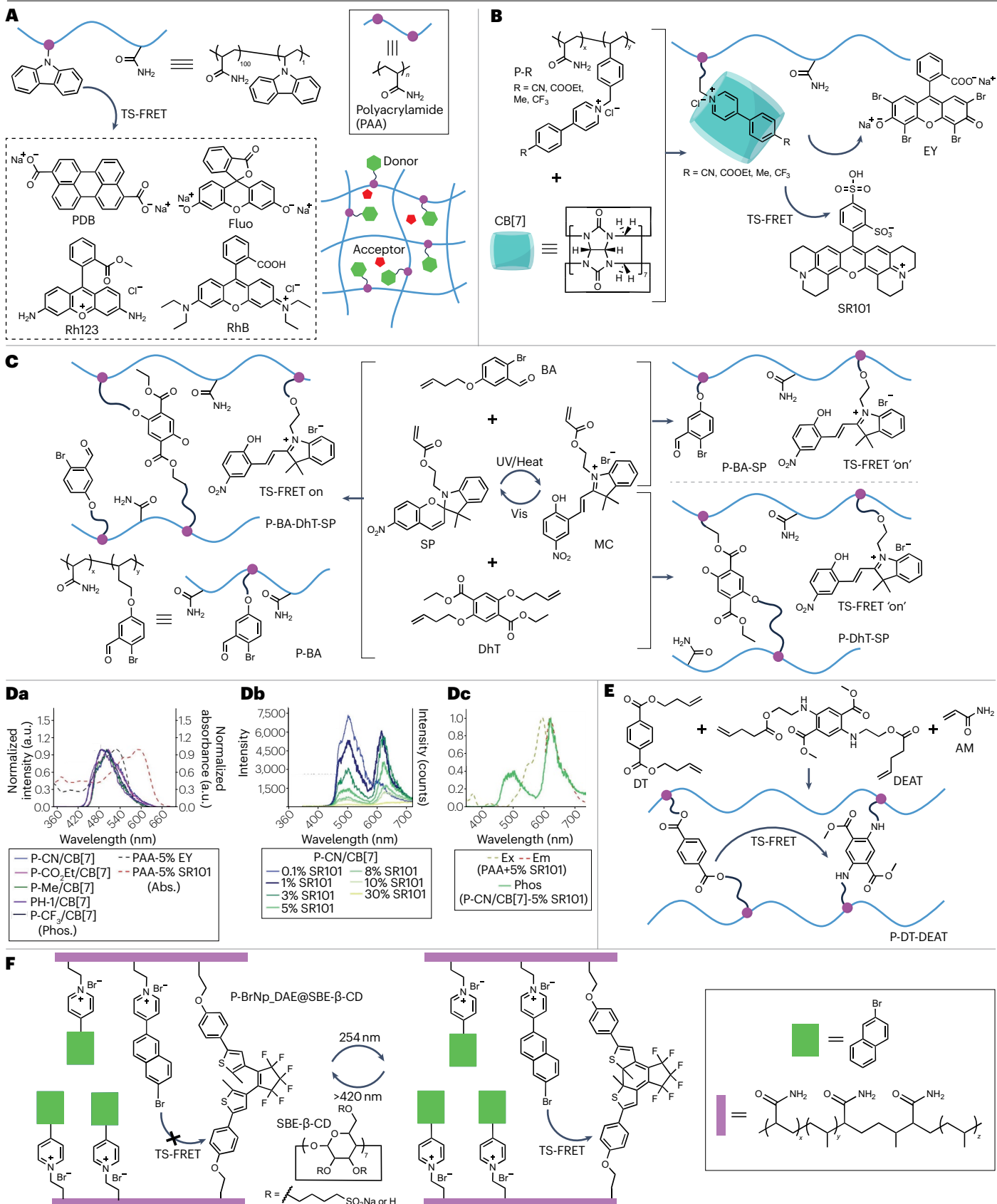


**Fig. 5 | Copolymerization-constructed solid-state supramolecular assemblies for PRET.**

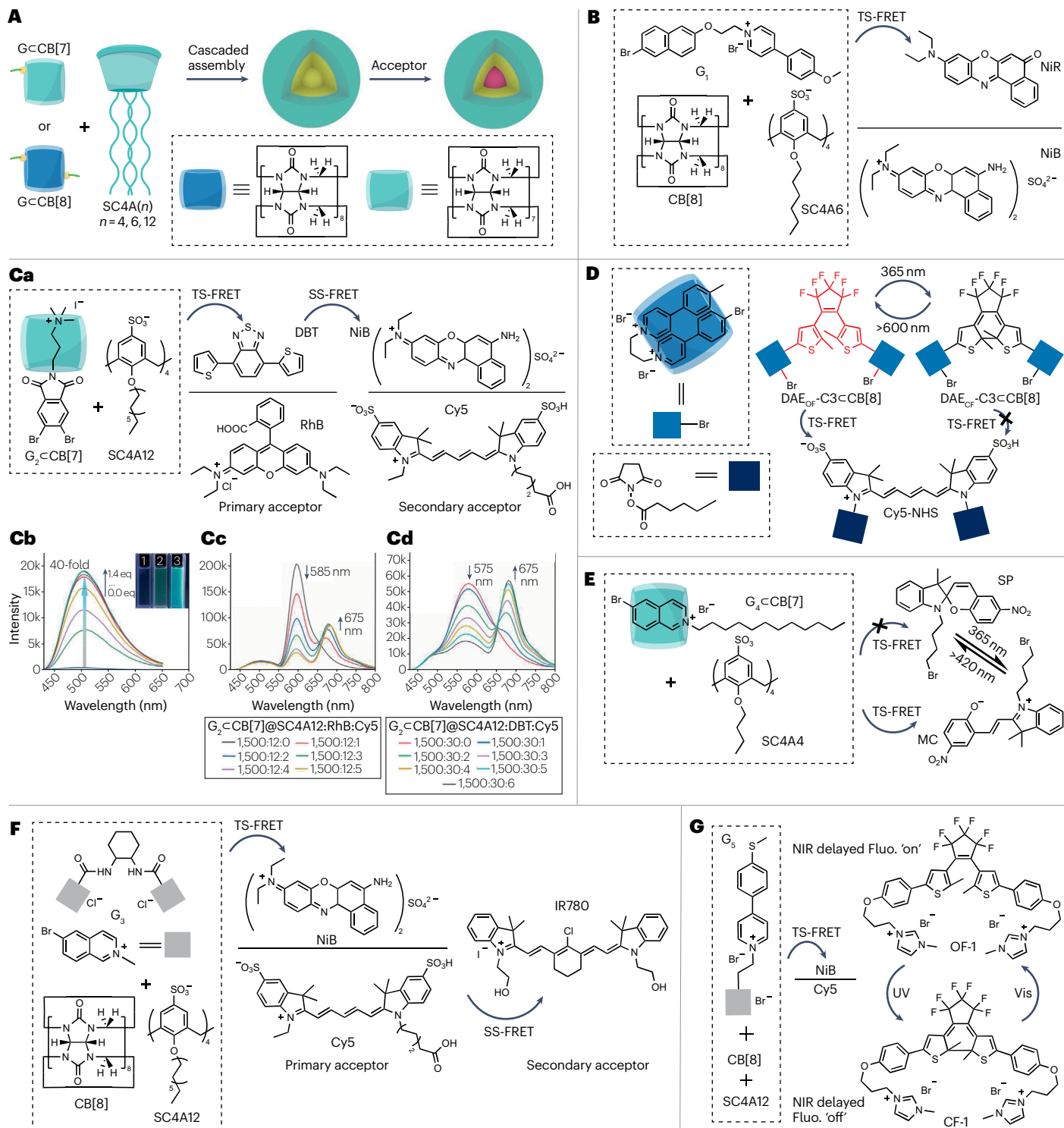
**A**, Schematic representation of a polymeric polyacrylamide (PAA) PRET systems by copolymerizing phosphorescence donors (green hexagons) and the fluorescence acceptors (red pentagons) shown in the inset: sodium 3,9-perylene dicarboxylate (PDB,  $\lambda_{em} = 502$  nm), sodium fluorescein (Fluo,  $\lambda_{em} = 560$  nm), Rhodamine 123 (Rh123,  $\lambda_{em} = 575$  nm) and Rhodamine B (RhB,  $\lambda_{em} = 618$  nm). **B**, Multicolour second-level phosphorescence assemblies based on 4-phenylpyridium derivatives-grafted acrylamide polymers (P-R), cucurbit[7]uril (CB[7]) and Eosin Y (EY,  $\lambda_{em} = 568$  nm) or Sulpharhodamine 101 (SR101,  $\lambda_{em} = 620$  nm). **C**, Irradiation (ultraviolet (UV), 365 nm and visible light) and heat-responsive multicolour conversion owing to copolymerization of photochromic spiropyran (SP,  $\lambda_{em} = 625$  nm), benzaldehyde (BA,  $\lambda_{em} = 510$  nm) and 2,5-dihydroxy terephthalate (DhT,  $\lambda_{em} = 520$  nm) with acrylamide (AM), including P-BA-SP, P-DhT-SP and P-BA-DhT-SP. **Da**, UV-vis absorption spectra of PAA containing SR101 or EY and phosphorescence spectra of P-R/CB[7].

**Db**, Delayed spectra of P-CN/CB[7] with varying SR101 concentrations. **Dc**, Excitation and photoluminescence spectra of PAA containing SR101 and a delayed spectrum of P-CN/CB[7]-SR101, combined indicating PRET processes. **E**, Tunable afterglows constructed from donor di(*but-3-en-1-yl*)terephthalate (DT) with blue-violet RTP emission ( $\lambda_{em} = 425$  nm) and acceptor dimethyl 2,5-bis((2-(pent-4-enoyloxy)ethyl)amino)terephthalate (DEAT) with orange fluorescence ( $\lambda_{em} = 580$  nm) through AM copolymerization at different feeding ratios (yielding P-DT-DEAT). **F**, Tunable ultra-strong white-light emission from sulfolbutylether- $\beta$ -cyclodextrin (SBE- $\beta$ -CD) and the copolymerization of 4-(6-bromonaphthalenyl)pyridine derivatives (BrNp) with diarylethene monomers (DAE) and AM (yielding P-BrNp-DAE) ('X' indicates that TS-FRET is not allowed.). Part **D** adapted with permission from ref. 113. Abs., absorption; FRET, Förster resonance energy transfer; MC, mecrocyanine; Phos., phosphorescence; PRET, phosphorescence resonance energy transfer; TS-FRET, triplet-to-singlet FRET.

phosphors, reduced non-radiative decay, and generated a hydrophobic environment to protect phosphors from water or dissolved oxygen species, thus achieving the highly efficient phosphorescence emission in solution state. SC4A[n] ( $n = 4, 6$  or  $12$ ) – the most commonly used class of multi-charged amphiphilic macrocycles – is composed of rigid cyclic pre-organized cavities, which allowed multiple functional units to assemble into compact supramolecular aggregates in which their structure and function were precisely controlled. The host-guest recognition of macrocyclic compounds can provide binding sites for energy donors or acceptors, improve the efficiency of energy transfer, and provide a convenient method for the construction of light-harvesting systems. In 2022, a unique supramolecular phosphorescence-capturing system via cascaded co-assembly taking advantage of CB[8] and SC4A6 under the macrocyclic and assembly confinement was reported<sup>123</sup> (Fig. 6B). CB[8] induced 'molecular folding' of bromonaphthalene-connected methoxyphenyl pyridinium salt ( $G_1$ ), in which the bromonaphthalene moiety folds back onto itself and stacks with the methoxyphenyl pyridinium moiety owing to the hydrophobic effects, ion-dipole interaction and  $\pi$ - $\pi$  stacking interaction, resulting in a 1:1 foldamer-like  $G_1$ C[B8] complex with an emerging RTP emission at 530 nm with a lifetime of 130.2  $\mu$ s. Furthermore,  $G_1$ C[B8] secondarily assembled with SC4A6 to give the  $G_1$ C[B8]@SC4A6 aggregate via electrostatic interactions between cationic guests and negatively charged sulfonic group and hydrophobic interactions mediated by the amphiphilic molecule of SC4A6. The formed aggregate exhibited a dramatic enhancement both in RTP emission intensity and lifetime (430.3  $\mu$ s). Benefiting from the fantastic RTP performance of  $G_1$ C[B8]@SC4A6, light-capturing platform can be created by loading a small amount of organic dyes such as Nile Red or Nile Blue (NiR and NiB, respectively) into the hydrophobic layer. The acquired RTP-capturing systems ( $G_1$ C[B8]@SC4A6/NiR and  $G_1$ C[B8]@SC4A6/NiB) with high efficiency ( $\Phi_{ET} = 84.4\%$  and  $76.3\%$ , respectively) and antenna effect (AE, 289.4 and 119.5, respectively) displayed delayed NIR emissive performance (635 and 675 nm, respectively). The phosphorescence-capturing system reveals the delayed NIR photoluminescence self-assembled structure in aqueous solution, which opens up for a feasible pathway for targeted NIR bioimaging in living cells.

Along with the development of phosphorescence energy transfer, RTP-based cascaded FRET has been put forward. To our knowledge, the photosynthetic light-harvesting systems usually involve a multi-step sequential singlet-singlet energy transfer process (cascading), rather than a one-step energy transfer. Cascaded FRET is a feasible

method to obtain larger Stokes shift and larger bathochromic-shift emission, which requires two energy transfer steps. The exploration of RTP-based cascaded FRET is greatly valuable for the development of more red-shifted long-lived NIR luminescence systems, which can be achieved by continuously introducing primary and secondary acceptors when there is a mismatch in the absorption spectrum between secondary receptors and the emission spectrum of the RTP energy donors. The successful fabrication of an ultrahigh supramolecular cascaded RTP-capturing system via the multivalent co-assembly strategy has been reported<sup>124</sup> (Fig. 6Ca). Specifically, the initial dibromophthalimide derivative ( $G_2$ ) produced very weak RTP emission at 505 nm induced by the host-guest interaction with CB[7] under the hydrophobic interaction and cation-dipole interactions. The cavity of CB[7] boosts ISC and reduces non-radiative transitions by restraining the vibration of  $G_2$ . In view of the inherent amphiphilicity, the resultant  $G_2$ C[B7] complex further co-assembled with the amphiphilic SC4A12 to prepare ternary supramolecular assembly of  $G_2$ C[B7]@SC4A12 with homogeneously spherical topology. Notably, the lifetime of  $G_2$ C[B7]@SC4A12 increased to 1.13 ms, and at the same time, the RTP emission intensity at 505 nm strengthened by 40-fold (Fig. 6Cb). After introducing the primary acceptor, RhB or 4,7-di(2-thienyl)-2,1,3-benzothiadiazole (DBT), energy transfer from the triplet of the phosphor to the singlet of the organic dyes took place with high  $\Phi_{ET}$  and AE. The microsecond lifetime of the organic dyes also indicated the occurrence of the TS-FRET process. Moreover, the efficient long-lived emission of primary acceptors provided the possibility for the second-stage energy transfer. With the addition of Cyanine 5 (Cy5) or NiB into  $G_2$ C[B7]@SC4A12/RhB or  $G_2$ C[B7]@SC4A12/DBT systems (Fig. 6Cc,d), an energy transfer process occurred from the singlet of the primary acceptor to the singlet of final acceptor in the assembly, ultimately yielding long-lived photoluminescence (83.4  $\mu$ s for  $G_2$ C[B7]@SC4A12/RhB/NiB, 83.1  $\mu$ s for  $G_2$ C[B7]@SC4A12/RhB/Cy5, 92.5  $\mu$ s for  $G_2$ C[B7]@SC4A12/DBT/NiB and 86.3  $\mu$ s for  $G_2$ C[B7]@SC4A12/DBT/Cy5). The systems were obtained in aqueous solution owing to the highly efficient cascaded PRET process. The multivalent supramolecular assembly with multicolour long-lived lifetime was shown to serve as a time-resolved fluorescent marker for cell imaging. To further extend the long-lived NIR emissive wavelength, they designed and synthesized the racemic 1,2-diaminocyclohexan-derived 6-bromoisoquinoline ( $G_3$ ), which generated a yellow phosphorescence emission at 555 nm confined by CB[8]<sup>125</sup> (Fig. 6F). Further co-assembly with SC4A12 enhanced its original phosphorescence emission intensity, and the phosphorescence



lifetime increased from 21.3  $\mu\text{s}$  to 364  $\mu\text{s}$ . Then, the  $G_3\text{CB}[8]@\text{SC4A12}$  assembly served as the energy donor to create the cascaded PRET system via successively introducing the primary acceptor, Cy5 or NiB, and the secondary acceptor, heptamethine cyanine (IR780). Based on this, the ultra-large Stokes shift ( $\approx 525$  nm) and long-lived NIR emission at

825 nm in aqueous solution were achieved, which was the first example of phosphorescence energy transfer system possessing long-emission wavelength (over 800 nm). The excellent long-lived NIR emission paved the way for developing phosphorescent supramolecular systems for imaging living cells in biological studies.

**Fig. 6 | Amphiphilic macrocyclic cascaded assemblies for PRET.**

**A**, Representation of cascaded PRET systems assembled by guests (G) with cucurbit[*n*]uril (CB[*n*], *n* = 7 or 8) and sulfonatocalix[4]arene (SC4A[*n*], *n* = 4, 6 or 12). **B**, Phosphorescence-capturing system based on the bromonaphthalene-connected methoxyphenyl pyridinium salt (G<sub>1</sub>), CB[8], SC4A6 and Nile red (NiR, λ<sub>em</sub> = 635 nm) or Nile blue (NiB, λ<sub>em</sub> = 675 nm). **Ca**, Supramolecular cascaded RTP-capturing system based on dibromophthalimide derivative (G<sub>2</sub>), CB[7], SC4A12, primary acceptor 4,7-di(2-thienyl)-2,1,3-benzothiadiazole (DBT, λ<sub>em</sub> = 575 nm) or Rhodamine B (RhB, λ<sub>em</sub> = 585 nm), and secondary acceptor NiB or Cyanine 5 (Cy5, λ<sub>em</sub> = 675 nm). **Cb**, Phosphorescence spectra of G<sub>2</sub>CB[7] with different SC4A12 concentrations in water, and photographs of G<sub>2</sub>, G<sub>2</sub>CB[7] and G<sub>2</sub>CB[7]@SC4A12 at 320 nm irradiation. **Cc,d**, Phosphorescence spectra of G<sub>2</sub>CB[7]@SC4A12/RhB/Cy5 or G<sub>2</sub>CB[7]@SC4A12:DBT: Cy5 at different donor-acceptor ratios. Intensity values: 1k = 1,000. **D**, Reversible supramolecular light switch for near-infrared (NIR) PRET based

on 4-(4-bromophenyl)-pyridinium connected to the open form of diarylethene via propyl (DAE<sub>of</sub>-C3), CB[8] and *N*-hydroxysuccinimide-modified Cy5 (Cy5-NHS). **E**, Phosphorescence-fluorescence supramolecular switch based on a dodecyl chain-modified 6-bromoisoquinoline derivative (G<sub>4</sub>), CB[7], SC4A4 and photochromic SP. Disallowed PRET is owing to absorption of non-fluorescent SP with no overlapping RTP emission of G<sub>4</sub>CB[7]@SC4A4 (indicated by 'X'). **F**, Ultra-large Stokes shift (≈525 nm) phosphorescence-capturing system based on racemic 1,2-diaminocyclohexan-derived 6-bromoisoquinoline (G<sub>3</sub>), CB[8], SC4A12, primary acceptor (NiB or Cy5) and secondary acceptor heptamethine cyanine (IR780, λ<sub>em</sub> = 825 nm). **G**, Phosphorescent energy transfer supramolecular switch based on 6-bromoisoquinoline-conjugated 4-(4-methylthiophenyl) pyridinium (G<sub>5</sub>), CB[8], SC4A12, acceptor dyes (NiB or Cy5) and diarylethene derivative in its open form (OF-1) and closed form (CF-1). Part **C** adapted with permission from ref. 124, Wiley. Fluo., fluorescence; FRET, Förster resonance energy transfer; NIR, near-infrared; SS-FRET, singlet-to-singlet FRET.

The above research mainly focused on the manufacture of static organic phosphorescence energy transfer. Dynamic energy transfer has attracted much attention owing to its stimulation response and reversibility. The spiropyran and diarylethene derivatives – as excellent optical molecular switches – have been utilized to construct dynamically reversible co-assembly supramolecular PRET systems. The construction of a photoresponsive PRET system is a crucial research topic for realizing tunable long-lived multicolour emission in aqueous solution. In 2022, a high-efficiency phosphorescence-fluorescence supramolecular switch was reported based on the cascaded assembly of dodecyl chain-modified 6-bromoisoquinoline derivative (G<sub>4</sub>)<sup>126</sup> (Fig. 6E). G<sub>4</sub> was used as the energy transfer donor, which showed an RTP emission signal at 540 nm under the confinement effect of CB[7]. Subsequently, the assembly-confinement effect mediated by SC4A4 greatly formed tight spherical nanoparticles and aided the RTP emission intensity and prolonged the phosphorescence lifetime from 50.1 μs to 1.80 ms. A photochromic SP derivative, as the photo-switch moiety, was loaded into the supramolecular nanoparticles. Nonfluorescent close-ring SP achieved light-controlled reversible conversion to the fluorescent open-ring macrocyanine (MC) form under alternating UV and visible photo-irradiation. When exposed to UV irradiation, the efficient light-driven PRET process occurred from the donor to the MC, resulting in a delayed red fluorescence at 635 nm with a lifetime of 83.8 μs. When the MC was transformed to the SP state when irradiated with visible light (>420 nm), the system displayed the original RTP emission at 540 nm. This phosphorescence and fluorescence supramolecular switch system was successfully applied for photo-controlled multicolour cell imaging. Moreover, the direct addition of the phosphorescent group onto the photo-switch molecule is another method to obtain photo-controlled PRET. By connecting the phosphorescent unit 4-(4-bromophenyl)-pyridinium with a photo-switching diarylethene skeleton in its open form via propyl (DAE<sub>of</sub>-C3)<sup>127</sup> (Fig. 6D), the obtained DAE<sub>of</sub>-C3 can produce phosphorescent emission in aqueous solution by CB[8] confinement in a dual-fold mode (DAE<sub>of</sub>-C3CB[8]). Of note, the DTE<sub>of</sub>-C3CB[8] showed efficient, reversible phosphorescence by the photochromism of the diarylethene unit form, its open form, to closed form (DAE<sub>cf</sub>-C3CB[8]) with a high phosphorescence quenching efficiency (99%). The phosphorescence switch could serve as the donor to transfer triplet energy to the organic dye *N*-hydroxysuccinimide-modified Cy5, achieving the photo-controlled energy transfer process and, thereby, rendering it suitable for information encryption and bioimaging. Additionally, diarylethene can

be introduced into the co-assembly to fabricate a phosphorescent light-harvesting supramolecular switch<sup>128</sup> (Fig. 6G). On the basis of the cascaded assembly confinement, the co-assembly composed of CB[8] encapsulating 6-bromoisoquinoline-conjugated 4-(4-methylthiophenyl) pyridinium (G<sub>5</sub>) and SC4A12 can serve as the phosphorescence energy donor centred on 605 nm. High spectral overlap between the phosphorescence emission of the above assembly G<sub>5</sub>CB[8]@SC4A12 and the absorption of the NiB and Cy5 enabled the efficient TS-FRET process. The doping of diarylethene derivatives (OF-1 or CF-1) triggered the photoluminescence quenching after irradiation by 365 nm light, which was restored when irradiated by 450 nm light. This concept has been applied to targeted imaging in HeLa cells and information encryption.

**Polymer-based co-assemblies**

Another feasible strategy of assembly confinement was polymer-based co-assembly with G<sub>2</sub>CB[7] or G<sub>2</sub>CB[8] complex, which diminishes the triplet non-radiative decay rate by creating a rigid environment with limited molecular vibration. Hence, some water-soluble polymers such as F127 and HA are used as the assembly units for inducing supramolecular self-assembly in aqueous solutions through noncovalent interactions such as electrostatic and hydrophobic interactions, effectuating the improved RTP emission (Fig. 7a). In 2020, a phosphorescence nanoprobe was made with delayed NIR emission based on PRET between *N,N*-bis(4-methoxyphenyl)-3-methyl-4-(4,4,5,5-tetramethyl-1,3,2-dioxaborolan-2-yl) aniline (mTPA) and a NIR fluorescent dye – silicon 2,3-naphthalocyanine bis(trihexylsilyloxy) (NCBS) – by leveraging the amphiphilic character of F127 through hydrophobic interactions and taking advantage of the top-down approach<sup>129</sup> (Fig. 7b). By transferring the short-wavelength RTP emission of mTPA to NIR fluorescent NCBS, the long-lived NIR afterglow at 780 nm was obtained. Afterglow images of living mice was captured with this phosphorescence nanoprobe with a high signal-to-noise ratio, effectively avoiding the biological auto-fluorescence, which provided a universal strategy to build afterglow probes with NIR emission for deep-tissue imaging.

Compared with the neutral amphiphilic copolymer F127, HA is a considerable negatively charged polysaccharide featuring good biocompatibility and cancer cell-targeted capacity, which directly co-assembles with cationic host-guest complexes via multiple interactions, and can be modified with functional guest molecules or macrocycles for further assembly to create high-performance RTP emission for PRET<sup>130</sup>. For example, a purely organic light-harvesting

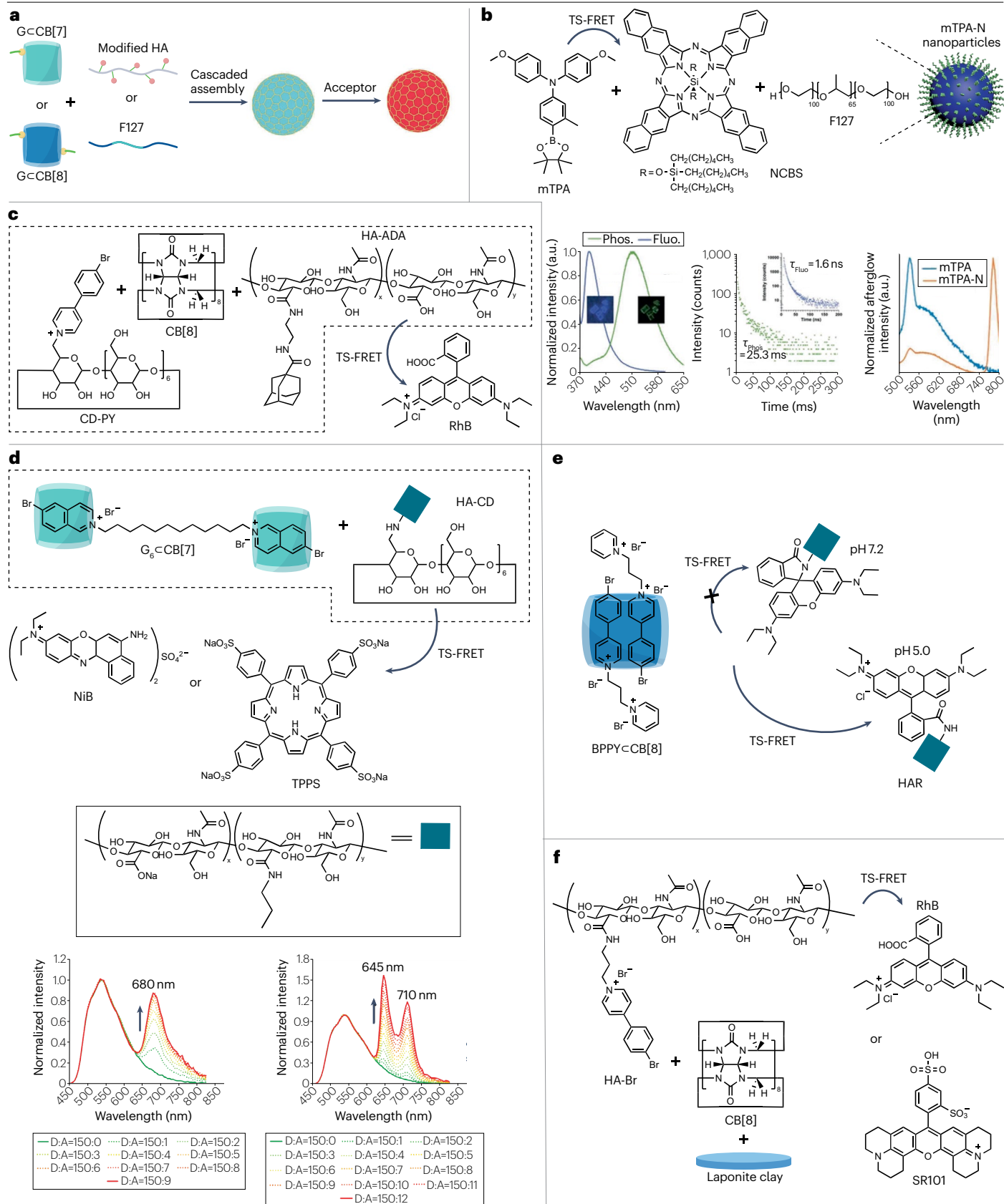


**Fig. 7 | Polymer-based co-assemblies for PRET.** **a**, Schematic representation of the fabrication of polymer-based co-assembled PRET systems with  $G_cCB[n]$  (cucurbit[ $n$ ]uril,  $n = 7$  or  $8$ ) complex and polymers such as modified hyaluronic acid (HA) or poly(ethylene glycol)-block-poly(propylene glycol)-block-poly(ethylene glycol) (F127). **b**, Phosphorescence nanoprobe (mTPA-N, blue sphere) with delayed NIR emission based on  $N,N$ -bis(4-methoxyphenyl)-3-methyl-4-(4,4,5,5-tetramethyl-1,3,2-dioxaborolan-2-yl) aniline (mTPA), silicon 2,3-naphthalocyanine bis(trihexylsilyloxy) (NCBS) and F127. Fluorescence (Fluo.) and phosphorescence (Phos.) spectra of mTPA crystals, as well as their lifetimes ( $\tau$ ), and afterglow spectra of mTPA and mTPA-N nanoparticles. **c**, Light-harvesting PRET based on 4-(4-bromophenyl)-pyridine-modified  $\beta$ -cyclodextrin (CD-PY), CB[8], Rhodamine B (RhB) and adamantine-modified HA (HA-ADA). **d**, Noncovalent polymerization-activated

PRET assembly based on dodecyl chain-bridged 6-bromoisoquinoline derivative ( $G_6$ ), CB[7],  $\beta$ -CD-modified HA (HA-CD) and NiR or tetrakis(4-sulfophenyl) porphyrin (TPPS). Phosphorescence spectra of  $G_6cCB[7]@HA-CD$  with different NiB (left) or TPPS (right) concentrations in water, normalized to the phosphorescence emission peak at 540 nm (D:A, ratio of donor to acceptor). **e**, In situ pH-activated PRET based on bromophenylpyridine derivative (BPPY), CB[8] and RhB-grafted HA (HAR). **f**, Ultralong PRET based on 4-(4-bromophenyl)-pyridine-modified HA (HA-Br), CB[8], Laponite clay (LP) and RhB or Sulpharhodamine 101 (SR101), in which HA-Br-CB[8]-LP presented a phosphorescence lifetime of up to 4.79 ms in water. Part **b** adapted with permission from ref. 129, Wiley. Part **d** adapted with permission from ref. 132, Wiley. PRET, phosphorescence resonance energy transfer; TS-FRET, triplet-to-singlet Förster resonance energy transfer.

PRET system in the aqueous solution was successfully constructed from adamantine-modified HA (HA-ADA), 4-(4-bromophenyl)-pyridine-modified  $\beta$ -cyclodextrin (CD-PY) and RhB<sup>131</sup> (Fig. 7c). In this system, the CB[8] was used to confine CD-PY for achieving the RTP emission as the energy donor in the aqueous solution, and then the acceptor RhB and HA-ADA were continuously introduced for further improving the photoluminescence intensity through supramolecular assembly confinement. In this co-assembly, RhB could be encapsulated by the cavity of CD, which further reduced the distance between donors and acceptors to promote TS-FRET, and HA served as the cancer-target agent. Additionally, the macrocycle-modified HA, such as  $\beta$ -CD-modified HA (HA-CD) can also be used to activate the TS-FRET process in aqueous solution via noncovalent polymerization<sup>132</sup> (Fig. 7d). Specifically, a dodecyl chain-bridged 6-bromoisoquinoline derivative ( $G_6$ ) and CB[7] can form a stable 1:2 complex with the weak RTP emission (59.0  $\mu$ s) at 540 nm under the macrocyclic confinement effect of CB[7]. Furthermore, the co-assembly between the 1:2 stable complex and HA-CD could exploit the secondary confinement effect because of electrostatic interaction which enhanced the original RTP emission with a prolonged lifetime to 581  $\mu$ s. Upon doping with two types of organic dyes, NiB and tetrakis(4-sulfophenyl)porphyrin, the energy transfer process took place within the supramolecular confinement assembly  $G_6cCB[7]@HA-CD$ . A long-lived NIR-emitting system was prepared via noncovalent polymerization, which was successfully applied in NIR imaging of living tumour cells. Moreover, PRET can be activated in situ by using a pH-responsive RhB as an acceptor to image cancer cells and discriminate from normal cells<sup>133</sup> (Fig. 7e). The bromophenylpyridine derivative co-assembled stepwise with CB[8] and RhB-grafted HA through noncovalent interactions, which formed a multivalent supramolecular assembly for the occurrence of TS-FRET. Interestingly, benefiting from the cyclolactam ring on-off reaction of RhB, and the targeting ability of HA, the TS-FRET process was activated in cancer cells under acidic pH conditions presenting red delayed fluorescence, and showed green RTP in normal cells, hence the effective discrimination of different types of cells. Additionally, the functional 4-(4-bromophenyl)-pyridine-modified HA can form a multivalent supramolecular assembly with CB[8] and Laponite clay (LP), which emitted a RTP emission with the ultralong lifetime up to 4.79 ms in aqueous solution<sup>134</sup>. By doping the above assemblies with organic dyes, such as RhB or SR101, efficient energy transfer was achieved with high transfer efficiency and ultrahigh antenna effect (Fig. 7f). Thus, a wide-range long-lived spectrum and white-light emissions in aqueous solution was obtained.

### Other co-assemblies

Phosphorescent carbon nanodots (CNDs) with ultralong lifetimes have attracted extensive research interest because of their low toxicity, small size and superior optical properties, and are ideal candidates as long-lived donors for PRET<sup>135,136</sup>. A water-soluble red afterglow nanocomposite has been reported based on the TS-FRET process between phosphorescent CNDs and RhB in a silica encapsulation layer. Benefiting from the long lifetime of phosphorescent CNDs (1.8 s) in the aqueous solution, RhB as the energy acceptor could produce a red afterglow via a delayed sensitization process, and a lifetime of 0.9 s – yielding a time-resolved in vivo afterglow imaging technique<sup>137</sup>. Similarly, a cascaded FRET system was constructed featuring multicolour long afterglow from green to yellow, to orange and then to red using the phosphorescent CDs and fluorescent dyes, which exhibited great potential in time-resolved and multicolour information encryption and bioimaging<sup>138</sup>. Additionally, on the basis of the PRET process between phosphorescent CNDs and Hg<sup>2+</sup>-responsive RhB derivatives, a proportional phosphorescent probe was established with high selectivity and sensitivity for Hg<sup>2+</sup> detection<sup>139</sup>.

As illustrated in Supplementary Tables 3 and 4, effective phosphorescence energy transfer platforms can be established in aqueous solution based on amphiphilic macrocycles or polymers. Firstly, macrocyclic compounds enhance ISC process and induce phosphorescence emission from the guests. Furthermore, owing to the stability of the triplet-state excitons in the hydrophobic microenvironment, the phosphorescence performance was notably improved by co-assembling with amphiphilic macrocycles or polymers. Additionally, the organic dyes tend to be loaded into the hydrophobic layer of the assembly, pulling the donor and acceptor closer together, providing the necessary conditions for PRET. The obtained aggregates possessed long-lived NIR emissions, which presented great potential in the NIR targeted imaging and even afterglow imaging in cells and tissues.

### PRET systems in hydrogels

Supramolecular hydrogels are three-dimensional cross-linked systems containing large amounts of water and composed of polymers through noncovalent interactions<sup>140,141</sup>. Compared with a solution, phosphorescent molecules can be directly involved in the gel formation, which can immobilize molecules and effectively isolate quenchers such as oxygen<sup>142–146</sup>. Studies have shown that supramolecular hydrogels can be used as new matrices for phosphorescence and then aid in the energy transfer from phosphorescent molecules, which is of importance for further development of soft materials. PRET systems in hydrogels are developed with LP as scaffold to anchor phosphors, or in situ phosphors

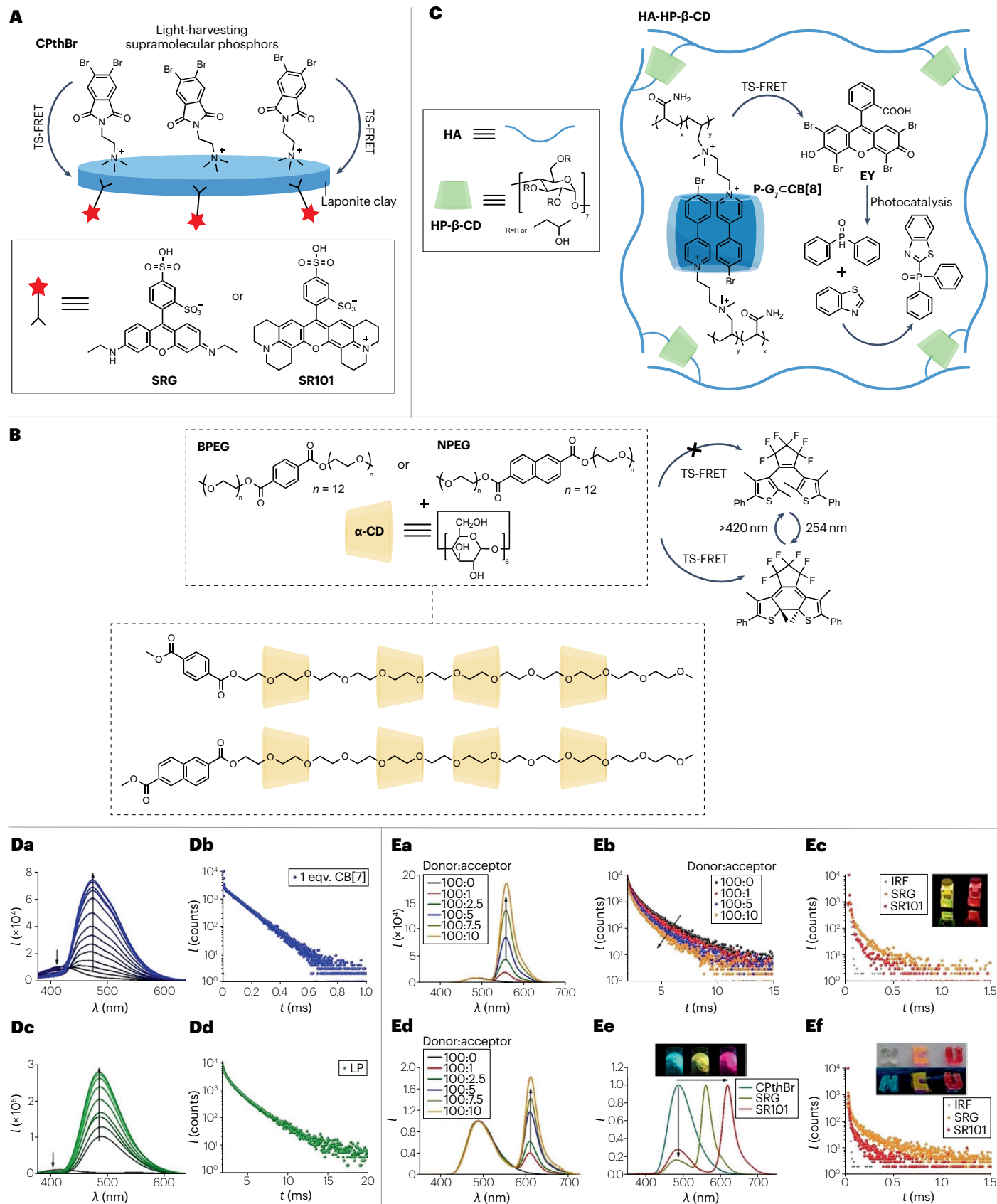


**Fig. 8 | Supramolecular hydrogels for PRET.** **A**, Light-harvesting supramolecular phosphors in solution and hydrogels based on cationic phthalimide derivative (CPthBr), Laponite clay (LP), and Sulpharhodamine G (SRG) or Sulpharhodamine 101 (SR101). **B**, Photo-controlled reversible phosphorescence supramolecular pseudopolyrotaxane based on benzene-modified polyethylene glycol (BPEG) derivatives and naphthalene-modified polyethylene glycol (NPEG) derivatives,  $\alpha$ -cyclodextrin ( $\alpha$ -CD) and a diarylethylene derivative. **C**, Double-network confined phosphorescence light-harvesting system for photocatalysis based on the copolymerization (P-G<sub>2</sub>) of dicationic vinylbromo-phenyl pyridine derivative (G<sub>2</sub>) with acrylamide, cucurbit[8]uril (CB[8]), hydroxypropyl- $\beta$ -CD-modified HA (HA-HP- $\beta$ -CD) and Eosin Y (EY). **Da–d**, Photoluminescence titration study of CPthBr with cucurbit[7]uril (CB[7]) or LP and the corresponding lifetime decay

plots. **Ea, b**, Normalized gated emission spectra of CPthBr-LP with different SRG concentrations (part **Ea**) and their lifetime decay plots at 490 nm in water (part **Eb**). **Ec**, Delayed fluorescence lifetimes for CPthBr-SRG-LP and CPthBr-SR101-LP in water (instrument response function (IRF)). Inset: photographs of CPthBr-SRG-LP and CPthBr-SR101-LP emission. **Ed**, Normalized gated emission spectra of CPthBr-LP with different SR101 contents. **Ee, f**, Normalized gated emission spectra (part **Ee**) and delayed fluorescence lifetimes (part **Ef**) for CPthBr-SRG-LP and CPthBr-SR101-LP in hydrogels. Inset: photographs of hydrogel structures and letters under visible light and 254 nm irradiation. Parts **D** and **E** adapted with permission from ref. 149, Wiley. HA, hyaluronic acid; TS-FRET, triplet-to-singlet Förster resonance energy transfer.

copolymerize with acrylamide. Both methods can provide confined microenvironment and allow the ordered assembly of donor–acceptor molecules to undergo PRET, which was applied for boosting the photocatalytic cross-coupling reaction and long-lived multicolour light-emitting soft material.

### Supramolecular hydrogels by noncovalent polymerization

Water-soluble LP nanoplates can serve as rigid scaffolds to control the molecular organization and stabilize triplet excitons owing to their unique structure and charge distribution with negatively charged surfaces and positively charged edges<sup>147,148</sup>. This allows them to provide anchor points and confined environments for organic molecules with complementary charges through electrostatic interactions. Such an organic-inorganic supramolecular scaffolds have been examined in order to induce the aqueous RTP emission of cationic phthalimide derivatives (CPthBr) and adjust the concentration to obtain supramolecular hydrogel materials<sup>149</sup> (Fig. 8A). In contrast to the host–guest complexation of CPthBr with CB[7] showing relatively weak RTP emission ( $\tau = 104 \mu\text{s}$ ) (Fig. 8Da, b), the negatively charged surface of LP nanoclays could anchor the cationic CPthBr to further improve its phosphorescence performance ( $\tau = 1.62 \text{ ms}$ ) (Fig. 8Dc, d). Subsequently, negatively charged acceptor molecules (SRG and SR101) were anchored to the edge of the LP, and delayed fluorescence from the acceptor molecule in both aqueous solution and the hydrogel state was achieved by effective PRET (Fig. 8Ea, b, d, e), possessing average lifetimes of 163.5  $\mu\text{s}$  and 60.4  $\mu\text{s}$  in solution (Fig. 8Ec) and 162  $\mu\text{s}$  and 55  $\mu\text{s}$  for hydrogels (Fig. 8Ef). This work provided a new approach to design multicolour long-lived phosphorescent amorphous hydrogel materials, especially for soft hydrogel. A polypseudorotaxane hydrogel has been prepared with only blue fluorescence by host–guest interactions between polyethylene glycol chain-modified bromophenylaldehyde derivatives and  $\alpha$ -cyclodextrin ( $\alpha$ -CD), and a polypseudorotaxane xerogel with white-light emission was also prepared because the fluorescence–phosphorescence dual emission property was obtained after lyophilization<sup>150</sup>. The rigid structure of the polypseudorotaxane xerogel network with hydrogen bonding and hydrophobic interactions could effectively suppress the non-radiative relaxation process of phosphor to give rise to efficient RTP emission. In addition, owing to the quenching effect of water, this polypseudorotaxane xerogel could be used in humidity sensing based on the reversible photoluminescence switch between white-light emission and blue fluorescence emission. Along this line, another two phosphorescent solid supramolecular pseudopolyrotaxanes were reported based on the host–guest interaction between benzene-modified or naphthalene-modified polyethylene glycol derivatives (BPEG or NPEG, respectively) and  $\alpha$ -CD.

The host molecule,  $\alpha$ -CD, interacts with the guest molecules BPEG or NPEG to form ordered channel-type crystalline pseudopolyrotaxane structures through hydrogen bonding and hydrophobic interactions, suppressing molecular vibrations and non-radiative decay, while promoting RTP emission and showing excitation-dependent multicolour afterglows<sup>151</sup> (Fig. 8B). Moreover, the diarylethylene derivative can be used to reversibly switch the long-lived phosphorescence on or off based on its photoisomerization process over several cycles under 254 nm and visible (>420 nm) irradiation in which the energy transfer occurred from phosphorescence to the closed form of DAE, proving its use in secure information storage and anti-counterfeiting.

### In situ copolymerization of supramolecular hydrogels

Another effective strategy for preparing phosphorescent supramolecular hydrogels is through in situ copolymerization<sup>152</sup>. For example, NIR RTP emissive supramolecular gels can be conveniently prepared by in situ copolymerizing acrylamide with iodine-substituted BODIPY dyes, ureidopyrimidone (UPy) and *N,N'*-methylenebisacrylamide, in which the self-complementary dimers formed by UPy moieties owing to the strong quadruple-hydrogen bonding interaction endowed the gels with excellent self-healing properties<sup>153</sup>. The synergistic effect of covalent and quadruple hydrogen bonds within the polymer gel provided a rigid confined environment for the phosphor and also helped shield it from the quenching effect of oxygen molecules. Also, a double-networked supramolecular PRET system was created based on the synergistic confinement of CB[8], encapsulating the dicationic vinylbromo-phenyl pyridine derivative (G<sub>2</sub>) through in situ copolymerization with acrylamide and hydroxypropyl- $\beta$ -CD-modified HA (HA-HP- $\beta$ -CD). This not only extended the phosphorescence lifetime from 442  $\mu\text{s}$  up to 5.17 ms but also lead to delayed fluorescence emission of EY when photosensitized by the phosphorescence<sup>154</sup> (Fig. 8C). In particular, HP- $\beta$ -CD can bind with the EY acceptor through host–guest interactions, thus promoting the efficient energy transfer from the triplet phosphorescence to the singlet EY. Benefiting from the long-lived photosensitizer, such systems exhibit an approximately 1.9 times enhancement in activity by cross-coupling reactions between benzothiazole and diphenyl phosphine oxide – in comparison with EY alone – which exhibited the promising potential of PRET systems for photochemical catalysis.

As summarized in Supplementary Tables 5 and 6, in contrast to solid and aqueous supramolecular PRET systems, the variety of the hydrogel-state supramolecular PRET systems should be further enriched, and their phosphorescent performances should also be even further improved. The reported methods for constructing hydrogel-state supramolecular PRET systems mainly include the non-covalent polymerization enabled by electrostatic interactions of LP or

host–guest interactions of cyclodextrins, and in situ copolymerization with acrylamide and phosphorescent monomers. These methods display millisecond-to-microsecond-level long-lived lifetimes and holds great application promises in advanced luminescent materials, photocatalytic synthesis and sensing fields.

## Concluding section

In this Review, we have systematically presented research advances regarding the purely organic supramolecular triplet-to-singlet PRET and triplet-to-singlet-to-singlet cascaded PRET in the solid amorphous state, aqueous solution and hydrogel, followed by a detailed discussion of their fabrication strategies, energy transfer mechanisms and wide range of applications such as information encryption, biomedical imaging and photocatalysis. The current supramolecular PRET systems mainly include the following construction approach; (1) polymer-mediated or copolymerization-constructed solid-state supramolecular assemblies, (2) aqueous amphiphilic macrocyclic cascaded or polymer-based supramolecular co-assemblies and (3) noncovalent polymerization or in situ copolymerization-constructed supramolecular hydrogels. The first strategy mainly utilizes the amorphous rigid polymer matrices (particularly PVA and PAA) through noncovalent or covalent interactions based on the direct incorporation of phosphorescent donors and fluorescent acceptors, or copolymerization with acrylamide. The second strategy is to leverage the water-soluble amphiphilic polymer, F127, or the macrocyclic hosts, SC4A[*n*], which assemble with phosphorescent donors by multivalent interactions in aqueous environments, and simultaneously provide a hydrophobic environment for loading fluorescent acceptors to promote the PRET process. The third strategy is to use the noncovalent polymerization based on multiple electrostatic interactions of LP scaffolds and host–guest interactions of CDs, as well as the in situ covalent copolymerization based on acrylamide and phosphors, producing self-standing soft supramolecular hydrogels with PRET behaviour. The mechanistic differences between the strategies are macrocyclic confinement caused by the tight inclusion and covalent or noncovalent assembly confinement for phosphorescence expansion, inhibiting non-radiative deactivation of phosphorescent molecules and protecting phosphorescence from external water or oxygen quenching. These steps also provide a confined environment for subsequent PRET. But, at the same time, other supramolecular assembly strategies still need to be developed based on the reported macrocycles and new various macrocyclic compounds, amphiphilic polymers and in situ copolymerization initiated by light and pH to promote their application in material design, information security and biomedical fields. Acrylamide has been a popular choice for copolymerization with functional groups to construct PRET systems owing to the water-soluble characteristic of PAA which is beneficial for large-area and large-scale production. Other monomers based on ionic liquid, zwitterionic or acrylic acid can be explored to further enrich the diversity of supramolecular PRET materials. Additionally, recent studies have shown that covalent organic frameworks can produce efficient RTP through covalent halogen doping or hydrogen bonding regulation strategies<sup>155,156</sup>, which may act as new matrices for PRET by further loading fluorescent acceptors into their highly ordered porous structures.

Despite the progress made on this topic, the design of high-performance purely organic PRET is still full of opportunities and challenges. The reported PRET process for acquiring long-lived luminous materials is owing to non-radiative energy transfer processes via FRET, in which the energy transfers from excited triplet donors to singlet

acceptors is based on the delayed sensitization process. Another strategy centred on the reabsorption process between triplet donors to singlet acceptors via the simple radiative energy transfer mechanism can also be considered to construct tunable long-persistent luminescence. Moreover, to compensate for the deficiencies of existing PRET hydrogels, noncovalent supramolecular interlocked crosslink structures, such as woven nodes, daisy chains and slide-ring polyrotaxane, can be introduced into the hydrogels to boost their dynamic adaptivity and mechanical properties. Also, creating circularly polarized PRET systems constitutes a considerable challenge, which might be overcome by using inherently chiral compounds (such as binaphthyl derivatives and twisted biphenyl derivatives) and chiral polymers as matrices (such as helical polyacetylenes and polyaminoacid) to endow achiral dyes with long-lived and circularly polarized luminescence. To further broaden the applications of purely organic PRET supramolecular assemblies, stimuli-responsive PRET systems are urgently needed, which can be created by using functional phosphors or fluorescent acceptors with specific responses to, for example, mechanical force, light, temperature, redox, enzymes, pH or biomarkers. Concerning bioimaging applications, novel supramolecular optical probes based on purely organic PRET that can be excited with two-photon, X-ray or chemiluminescence sources for high-contrast and deep-tissue afterglow imaging in the second near-infrared window (NIR-II, 1000–1700 nm) still need to be explored, owing to the considerable importance of precise measurements related to molecular dynamics of biological materials and accurate diagnoses of diseases.

Published online: 22 November 2023

## References

- Guo, J., Yang, C. & Zhao, Y. Long-lived organic room-temperature phosphorescence from amorphous polymer systems. *Acc. Chem. Res.* **55**, 1160–1170 (2022).
- Shi, H. et al. Ultralong organic phosphorescence: from material design to applications. *Acc. Chem. Res.* **55**, 3445–3459 (2022).
- Zhang, T. et al. Molecular engineering for metal-free amorphous materials with room-temperature phosphorescence. *Angew. Chem. Int. Ed. Engl.* **59**, 11206–11216 (2020).
- Yang, J., Fang, M. & Li, Z. Stimulus-responsive room temperature phosphorescence materials: internal mechanism, design strategy, and potential application. *Acc. Mater. Res.* **2**, 644–654 (2021).
- Garain, S. et al. Arylene diimide phosphors: aggregation modulated twin room temperature phosphorescence from pyromellitic diimides. *Angew. Chem. Int. Ed. Engl.* **60**, 12323–12327 (2021).
- Xie, Z. et al. Wide-range lifetime-tunable and responsive ultralong organic phosphorescent multi-host/guest system. *Nat. Commun.* **12**, 3522 (2021).
- Li, W. et al. A dish-like molecular architecture for dynamic ultralong room-temperature phosphorescence through reversible guest accommodation. *Nat. Commun.* **13**, 7423 (2022).
- Liu, X. Q. et al. Monochromophore-based phosphorescence and fluorescence from pure organic assemblies for ratiometric hypoxia detection. *Angew. Chem. Int. Ed. Engl.* **59**, 23456–23460 (2020).
- He, Z. et al. Achieving persistent, efficient, and robust room-temperature phosphorescence from pure organics for versatile applications. *Adv. Mater.* **31**, e1807222 (2019).
- Ma, Y. J., Fang, X., Xiao, G. & Yan, D. Dynamic manipulating space-resolved persistent luminescence in core-shell MOFs heterostructures via reversible photochromism. *Angew. Chem. Int. Ed.* **61**, e202114100 (2022).
- Wang, Z. et al. Four-in-one stimulus-responsive long-lived luminescent systems based on pyrene-doped amorphous polymers. *Angew. Chem. Int. Ed.* **61**, e202203254 (2022).
- Yang, Y. et al. Tunable photoresponsive behaviors based on triphenylamine derivatives: the pivotal role of  $\pi$ -conjugated structure and corresponding application. *Adv. Mater.* **33**, e2104002 (2021).
- Cai, S. et al. Ultralong organic phosphorescent foams with high mechanical strength. *J. Am. Chem. Soc.* **143**, 16256–16263 (2021).
- Wang, T. et al. Aggregation-induced dual-phosphorescence from organic molecules for nondoped light-emitting diodes. *Adv. Mater.* **31**, 1904273 (2019).
- Gong, Y. et al. Achieving persistent room temperature phosphorescence and remarkable mechanochromism from pure organic luminogens. *Adv. Mater.* **27**, 6195–6201 (2015).

16. Wang, H. et al. Visualization and manipulation of solid-state molecular motions in cocrystallization processes. *J. Am. Chem. Soc.* **143**, 9468–9477 (2021).
17. Wang, X. F. et al. Pure organic room temperature phosphorescence from unique micelle-assisted assembly of nanocrystals in water. *Adv. Funct. Mater.* **30**, 1907282 (2020).
18. Yang, J. et al. The influence of the molecular packing on the room temperature phosphorescence of purely organic luminogens. *Nat. Commun.* **9**, 840 (2018).
19. Bolton, O., Lee, K., Kim, H. J., Lin, K. Y. & Kim, J. Activating efficient phosphorescence from purely organic materials by crystal design. *Nat. Chem.* **3**, 205–210 (2011).
20. Yuan, W. Z. et al. Crystallization-induced phosphorescence of pure organic luminogens at room temperature. *J. Phys. Chem. C* **114**, 6090–6099 (2010).
21. Gu, L. et al. Color-tunable ultralong organic room temperature phosphorescence from a multicomponent copolymer. *Nat. Commun.* **11**, 944 (2020).
22. Gu, L. et al. Circularly polarized organic room temperature phosphorescence from amorphous copolymers. *J. Am. Chem. Soc.* **143**, 18527–18535 (2021).
23. Zhang, Z. Y. et al. A synergistic enhancement strategy for realizing ultralong and efficient room-temperature phosphorescence. *Angew. Chem. Int. Ed. Engl.* **59**, 18748–18754 (2020).
24. Wu, H. et al. Molecular phosphorescence in polymer matrix with reversible sensitivity. *ACS Appl. Mater. Interfaces* **12**, 20765–20774 (2020).
25. Zhang, Y. et al. Ultraviolet irradiation-responsive dynamic ultralong organic phosphorescence in polymeric systems. *Nat. Commun.* **12**, 2297 (2021).
26. Su, Y. et al. Excitation-dependent long-life luminescent polymeric systems under ambient conditions. *Angew. Chem. Int. Ed. Engl.* **59**, 9967–9971 (2020).
27. Wang, Z. et al. Accessing excitation- and time-responsive afterglows from aqueous processable amorphous polymer films through doping and energy transfer. *Adv. Mater.* **34**, 2202182 (2022).
28. Wu, H. et al. Tailoring noncovalent interactions to activate persistent room-temperature phosphorescence from doped polyacrylonitrile films. *Adv. Funct. Mater.* **31**, 2101656 (2021).
29. Ding, B. et al. Engendering persistent organic room temperature phosphorescence by trace ingredient incorporation. *Sci. Adv.* **7**, eabf9668 (2021).
30. Zhou, W. L. et al. Ultralong purely organic aqueous phosphorescence supramolecular polymer for targeted tumor cell imaging. *Nat. Commun.* **11**, 4655 (2020).
31. Zhu, W., Xing, H., Li, E., Zhu, H. & Huang, F. Room-temperature phosphorescence in the amorphous state enhanced by copolymerization and host-guest complexation. *Macromolecules* **55**, 9802–9809 (2022).
32. Wang, J., Huang, Z., Ma, X. & Tian, H. Visible-light-excited room-temperature phosphorescence in water by cucurbit[8]uril-mediated supramolecular assembly. *Angew. Chem. Int. Ed. Engl.* **59**, 9928–9933 (2020).
33. Zhang, X. et al. Ultralong UV/mechano-excited room temperature phosphorescence from purely organic cluster excitons. *Nat. Commun.* **10**, 5161 (2019).
34. Li, D. et al. Amorphous metal-free room-temperature phosphorescent small molecules with multicolor photoluminescence via a host-guest and dual-emission strategy. *J. Am. Chem. Soc.* **140**, 1916–1923 (2018).
35. Zhang, Z. Y., Chen, Y. & Liu, Y. Efficient room-temperature phosphorescence of a solid-state supramolecule enhanced by cucurbit[6]uril. *Angew. Chem. Int. Ed. Engl.* **58**, 6028–6032 (2019).
36. Yu, X. et al. Room-temperature phosphorescent gamma-cyclodextrin-cucurbit[6]uril-cowheeled [4]rotaxanes for specific sensing of tryptophan. *Chem. Commun.* **55**, 3156–3159 (2019).
37. Dou, X. et al. Color-tunable, excitation-dependent, and time-dependent afterglows from pure organic amorphous polymers. *Adv. Mater.* **32**, e2004768 (2020).
38. Li, D., Yang, J., Fang, M., Tang, B. Z. & Li, Z. Stimulus-responsive room temperature phosphorescence materials with full-color tunability from pure organic amorphous polymers. *Sci. Adv.* **8**, eab18392 (2022).
39. Fan, Y. et al. Mobile phone flashlight-excited red afterglow bioimaging. *Adv. Mater.* **34**, 2201280 (2022).
40. Sun, S., Ma, L., Wang, J., Ma, X. & Tian, H. Red-light excited efficient metal-free near-infrared room-temperature phosphorescent films. *Natl. Sci. Rev.* **9**, nwab085 (2022).
41. Xiao, F. et al. Guest-host doped strategy for constructing ultralong-lifetime near-infrared organic phosphorescence materials for bioimaging. *Nat. Commun.* **13**, 186 (2022).
42. Pan, Y. et al. Highly efficient TADF-type organic afterglow of long emission wavelengths. *Adv. Funct. Mater.* **32**, 2110207 (2022).
43. Li, Z., Han, Y. & Wang, F. Compartmentalization-induced phosphorescent emission enhancement and triplet energy transfer in aqueous medium. *Nat. Commun.* **10**, 3735 (2019).
44. Katsuruda, Y., Hirata, S., Totani, K., Watanabe, T. & Vacha, M. Photoreversible on-off recording of persistent room-temperature phosphorescence. *Adv. Opt. Mater.* **3**, 1726–1737 (2015).
45. Hoshi, M., Nishiyabu, R., Hayashi, Y., Yagi, S. & Kubo, Y. Room-temperature phosphorescence-active boronate particles: characterization and ratiometric afterglow-sensing behavior by surface grafting of Rhodamine B. *Chem. Asian J.* **15**, 787–795 (2020).
46. Ning, Y. et al. Ultralong organic room-temperature phosphorescence of electron-donating and commercially available host and guest molecules through efficient Förster resonance energy transfer. *Sci. China Chem.* **64**, 739–744 (2021).
47. Mu, Y. et al. Reversible and continuous color-tunable persistent luminescence of metal-free organic materials by “self”-interface energy transfer. *ACS Appl. Mater. Interfaces* **12**, 5073–5080 (2020).
48. Peng, H. Q. et al. Biological applications of supramolecular assemblies designed for excitation energy transfer. *Chem. Rev.* **115**, 7502–7542 (2015).
49. Bennett, R. G. Radiationless intermolecular energy transfer. I. Singlet→singlet transfer. *J. Chem. Phys.* **41**, 3037–3040 (1964).
50. Scholes, G. D. Long-range resonance energy transfer in molecular systems. *Annu. Rev. Phys. Chem.* **54**, 57–87 (2003).
51. Förster, T. 10th Spiers Memorial Lecture. Transfer mechanisms of electronic excitation. *Discuss. Faraday Soc.* **27**, 7–17 (1959).
52. Gao, R., Mei, X., Yan, D., Liang, R. & Wei, M. Nano-photosensitizer based on layered double hydroxide and isophthalic acid for singlet oxygenation and photodynamic therapy. *Nat. Commun.* **9**, 2798 (2018).
53. Tanner, P. A., Zhou, L., Duan, C. & Wong, K. L. Misconceptions in electronic energy transfer: bridging the gap between chemistry and physics. *Chem. Soc. Rev.* **47**, 5234–5265 (2018).
54. Zhao, W. et al. Boosting the efficiency of organic persistent room-temperature phosphorescence by intramolecular triplet-triplet energy transfer. *Nat. Commun.* **10**, 1595 (2019).
55. Li, G. et al. Organic supramolecular zippers with ultralong organic phosphorescence by a Dexter energy transfer mechanism. *Angew. Chem. Int. Ed. Engl.* **61**, e202113425 (2022).
56. Kislov, D. A. & Kucherenko, M. G. Nonradiative triplet-singlet transfer of electronic excitation energy between dye molecules in the vicinity of the silver-film surface. *Opt. Spectrosc.* **117**, 784–791 (2014).
57. Ermolaev, V. L. Energy transfer in organic systems involving the triplet state III. Rigid solutions and crystals. *Sov. Phys. Uspekhi* **6**, 333–358 (1963).
58. Wasserberg, D., Meskers, S. J. & Janssen, R. J. Phosphorescent resonant energy transfer between iridium complexes. *J. Phys. Chem. A* **111**, 1381–1388 (2007).
59. Volyniuk, D. et al. Highly efficient blue organic light-emitting diodes based on intermolecular triplet-singlet energy transfer. *J. Phys. Chem. C* **117**, 22538–22544 (2013).
60. Ma, X., Wang, J. & Tian, H. Assembling-induced emission: an efficient approach for amorphous metal-free organic emitting materials with room-temperature phosphorescence. *Acc. Chem. Res.* **52**, 738–748 (2019).
61. Ma, X. K. & Liu, Y. Supramolecular purely organic room-temperature phosphorescence. *Acc. Chem. Res.* **54**, 3403–3414 (2021).
62. Zhu, X., Wang, J.-X., Niu, L.-Y. & Yang, Q.-Z. Aggregation-induced emission materials with narrowed emission band by light-harvesting strategy: fluorescence and chemiluminescence imaging. *Chem. Mater.* **31**, 3573–3581 (2019).
63. Guo, S., Song, Y., He, Y., Hu, X. Y. & Wang, L. Highly efficient artificial light-harvesting systems constructed in aqueous solution based on supramolecular self-assembly. *Angew. Chem. Int. Ed. Engl.* **57**, 3163–3167 (2018).
64. Hao, M. et al. A supramolecular artificial light-harvesting system with two-step sequential energy transfer for photochemical catalysis. *Angew. Chem. Int. Ed. Engl.* **59**, 10095–10100 (2020).
65. Song, Q. et al. Efficient artificial light-harvesting system based on supramolecular peptide nanotubes in water. *J. Am. Chem. Soc.* **143**, 382–389 (2021).
66. Zhao, W., He, Z. & Tang, B. Z. Room-temperature phosphorescence from organic aggregates. *Nat. Rev. Mater.* **5**, 869–885 (2020).
67. Barman, D. et al. Review on recent trends and prospects in  $\pi$ -conjugated luminescent aggregates for biomedical applications. *Aggregate* **3**, e172 (2022).
68. Börjesson, K. et al. Multiplicity conversion based on intramolecular triplet-to-singlet energy transfer. *Sci. Adv.* **5**, eaaw5978 (2019).
69. Cravencio, A., Ye, C., Grafenstein, J. & Börjesson, K. Interplay between Förster and Dexter energy transfer rates in isomeric donor-bridge-acceptor systems. *J. Phys. Chem. A* **124**, 7219–7227 (2020).
70. Maliwal, B. P., Gryczynski, Z. & Lakowicz, J. R. Long-wavelength long-lifetime luminescences. *Anal. Chem.* **73**, 4277–4285 (2001).
71. D’Andrade, B. W. et al. High-efficiency yellow double-doped organic light-emitting devices based on phosphor-sensitized fluorescence. *Appl. Phys. Lett.* **79**, 1045–1047 (2001).
72. Chidrala, S. et al. Pyrene-oxadiazoles for organic light-emitting diodes: triplet to singlet energy transfer and role of hole-injection/hole-blocking materials. *J. Org. Chem.* **81**, 603–614 (2016).
73. Sun, Y. et al. Management of singlet and triplet excitons for efficient white organic light-emitting devices. *Nature* **440**, 908–912 (2006).
74. Tavares, I. G., Enkvist, E., Kaimre, J., Uri, A. & Dias, F. B. Intramolecular interchromophore singlet-singlet and triplet-singlet energy transfer in a metal-free donor-acceptor emitter. *J. Lumin.* **237**, 118183 (2021).
75. Ibrayev, N., Seliverstova, E., Temirbayeva, D. & Ishchenko, A. Plasmon effect on simultaneous singlet-singlet and triplet-singlet energy transfer. *J. Lumin.* **251**, 119203 (2022).
76. Baldo, M. A., Thompson, M. E. & Forrest, S. R. High-efficiency fluorescent organic light-emitting devices using a phosphorescent sensitizer. *Nature* **403**, 750–753 (2000).
77. Xia, D. et al. Functional supramolecular polymeric networks: the marriage of covalent polymers and macrocycle-based host-guest interactions. *Chem. Rev.* **120**, 6070–6123 (2020).
78. Liu, Z. & Liu, Y. Multicharged cyclodextrin supramolecular assemblies. *Chem. Soc. Rev.* **51**, 4786–4827 (2022).
79. Nie, H., Wei, Z., Ni, X. L. & Liu, Y. Assembly and applications of macrocyclic-confinement-derived supramolecular organic luminescent emissions from cucurbiturils. *Chem. Rev.* **122**, 9032–9077 (2022).

80. Gao, R., Yan, D. & Duan, X. Layered double hydroxides-based smart luminescent materials and the tuning of their excited states. *Cell Rep. Phys. Sci.* **2**, 100536 (2021).
81. Yan, X. et al. Recent advances on host-guest material systems toward organic room temperature phosphorescence. *Small* **18**, e2104073 (2022).
82. Zhou, W. L., Lin, W., Chen, Y. & Liu, Y. Supramolecular assembly confined purely organic room temperature phosphorescence and its biological imaging. *Chem. Sci.* **13**, 7976–7989 (2022).
83. Guo, S. et al. Recent progress in pure organic room temperature phosphorescence of small molecular host-guest systems. *ACS Mater. Lett.* **3**, 379–397 (2021).
84. Sun, H., Shen, S. & Zhu, L. Photo-stimuli-responsive organic room-temperature phosphorescent materials. *ACS Mater. Lett.* **4**, 1599–1615 (2022).
85. Sun, H. & Zhu, L. Achieving purely organic room temperature phosphorescence in aqueous solution. *Aggregate* **4**, e253 (2022).
86. Zhang, Y. et al. Cross-linked polyphosphazene nanospheres boosting long-lived organic room-temperature phosphorescence. *J. Am. Chem. Soc.* **144**, 6107–6117 (2022).
87. Li, J. J., Chen, Y., Yu, J., Cheng, N. & Liu, Y. A supramolecular artificial light-harvesting system with an ultrahigh antenna effect. *Adv. Mater.* **29**, 1701905 (2017).
88. Su, Y. et al. Ultralong room temperature phosphorescence from amorphous organic materials toward confidential information encryption and decryption. *Sci. Adv.* **4**, eaas9732 (2018).
89. Wu, H. et al. Achieving amorphous ultralong room temperature phosphorescence by coassembling planar small organic molecules with polyvinyl alcohol. *Adv. Funct. Mater.* **29**, 1807243 (2019).
90. Zhang, Y. et al. Large-area, flexible, transparent, and long-lived polymer-based phosphorescence films. *J. Am. Chem. Soc.* **143**, 13675–13685 (2021).
91. Kuila, S. & George, S. J. Phosphorescence energy transfer: ambient afterglow fluorescence from water-processable and purely organic dyes via delayed sensitization. *Angew. Chem. Int. Ed. Engl.* **59**, 9393–9397 (2020).  
**This work reports the ambient red afterglow in water-processable and flexible poly(vinylalcohol) films via a delayed sensitization process.**
92. Wang, D. et al. Achieving color-tunable and time-dependent organic long persistent luminescence via phosphorescence energy transfer for advanced anti-counterfeiting. *Adv. Funct. Mater.* **33**, 2208895 (2023).  
**This study establishes the structure–property relationship between similar isomers and phosphorescence performance, and presents tunable solid-state long persistent luminescence via phosphorescence energy transfer.**
93. Sun, W., Shi, B., Xia, Z. & Lv, C. Visible-light-excited long-lived organic room-temperature phosphorescence of phenanthroline derivatives in PVA matrix by H-bonding interaction for security applications. *Mater. Today Chem.* **27**, 101297 (2023).
94. Xiong, S. et al. Achieving tunable organic afterglow and UV irradiation-responsive ultralong room-temperature phosphorescence from pyridine-substituted triphenylamine derivatives. *Adv. Mater.* **35**, 2301874 (2023).
95. Wei, P. et al. New wine in old bottles: prolonging room-temperature phosphorescence of crown ethers by supramolecular interactions. *Angew. Chem. Int. Ed. Engl.* **59**, 9293–9298 (2020).
96. Wang, H. J. et al. Noncovalent bridged bis(coumarin-24-crown-8) phosphorescent supramolecular switch. *Adv. Opt. Mater.* **10**, 2201903 (2022).
97. Kanakubo, M., Yamamoto, Y. & Kubo, Y. Room-temperature phosphorescence of thiophene boronate ester-cross linked polyvinyl alcohol; a triplet-to-singlet FRET-induced multi-color afterglow luminescence with Sulforhodamine B. *Bull. Chem. Soc. Jpn* **94**, 1204–1209 (2021).
98. Tian, R. et al. Large-scale preparation for efficient polymer-based room-temperature phosphorescence via click chemistry. *Sci. Adv.* **6**, eaaz6107 (2020).
99. Li, D. et al. Completely aqueous processable stimulus responsive organic room temperature phosphorescence materials with tunable afterglow color. *Nat. Commun.* **13**, 347 (2022).  
**This work introduces B–O covalent bond into poly(vinylalcohol) matrix to facilitate phosphorescence emission and realizes stimulus-responsive tunable afterglow.**
100. Lin, F. et al. Stepwise energy transfer: near-infrared persistent luminescence from doped polymeric systems. *Adv. Mater.* **34**, e2108333 (2022).  
**This paper describes a universal method to realize near-infrared persistent luminescence via stepwise energy transfer.**
101. Kirch, A., Gmelch, M. & Reineke, S. Simultaneous singlet-singlet and triplet-singlet Förster resonance energy transfer from a single donor material. *J. Phys. Chem. Lett.* **10**, 310–315 (2019).  
**This work reports the simultaneous singlet-to-singlet and triplet-to-singlet Förster resonance energy transfer from a biluminescent donor molecule in an amorphous polymeric film.**
102. Wang, X. et al. Reversible photoswitching between fluorescence and room temperature phosphorescence by manipulating excited state dynamics in molecular aggregates. *Angew. Chem. Int. Ed. Engl.* **61**, e202114264 (2022).  
**This work demonstrates a photoreversible fluorescence and room-temperature phosphorescence switching based on a photo-controlled triplet-to-singlet Förster resonance energy transfer.**
103. Zhao, Y. et al. Visible light activated organic room-temperature phosphorescence based on triplet-to-singlet Förster-resonance energy transfer. *Adv. Opt. Mater.* **10**, 2102701 (2022).
104. Zheng, X. et al. A processable, scalable, and stable full-color ultralong afterglow system based on heteroatom-free hydrocarbon doped polymers. *Mater. Horiz.* **10**, 197–208 (2023).
105. Wang, C. et al. Photo-induced dynamic room temperature phosphorescence based on triphenyl phosphonium containing polymers. *Adv. Funct. Mater.* **32**, 2111941 (2022).
106. Wu, M. et al. Two-component design strategy: achieving intense organic afterglow and diverse functions in coronene-matrix systems. *J. Phys. Chem. C* **125**, 26986–26998 (2021).
107. Hayashi, K., Fukasawa, K., Yamashita, T. & Hirata, S. Rational design of a triplet afterglow sensitizer allowing for bright long-wavelength afterglow room-temperature emission. *Chem. Mater.* **34**, 1627–1637 (2022).
108. Gao, R. & Yan, D. Layered host-guest long-afterglow ultrathin nanosheets: high-efficiency phosphorescence energy transfer at 2D confined interface. *Chem. Sci.* **8**, 590–599 (2017).
109. Ma, X., Xu, C., Wang, J. & Tian, H. Amorphous pure organic polymers for heavy-atom-free efficient room-temperature phosphorescence emission. *Angew. Chem. Int. Ed. Engl.* **57**, 10854–10858 (2018).
110. Lin, X., Wang, J., Ding, B., Ma, X. & Tian, H. Tunable-emission amorphous room-temperature phosphorescent polymers based on thermoreversible dynamic covalent bonds. *Angew. Chem. Int. Ed. Engl.* **60**, 3459–3463 (2021).
111. Peng, H. et al. On-demand modulating afterglow color of water-soluble polymers through phosphorescence FRET for multicolor security printing. *Sci. Adv.* **8**, eabk2925 (2022).  
**This study develops a full-colour organic ultralong phosphorescence materials with multicolour-emitting afterglow which are successfully used for multicolour security printing.**
112. Zhang, X. et al. Multicolor hyperafterglow from isolated fluorescence chromophores. *Nat. Commun.* **14**, 475 (2023).
113. Xu, W. W. et al. Tunable second-level room-temperature phosphorescence of solid supramolecules between acrylamide-phenylpyridium copolymers and cucurbit[7]uril. *Angew. Chem. Int. Ed. Engl.* **61**, e202115265 (2022).  
**This work reports tunable second-level phosphorescence based on acrylamide copolymerization and host-guest interaction.**
114. Gui, H., Huang, Z., Yuan, Z. & Ma, X. Ambient white-light afterglow emission based on triplet-to-singlet Förster resonance energy transfer. *CCS Chem.* **4**, 173–181 (2022).  
**This work reports the tunable luminescent copolymers based on two simple single-benzene-based molecules which show multicolour afterglow including ambient white afterglow.**
115. Gu, F., Ding, B., Ma, X. & Tian, H. Tunable fluorescence and room-temperature phosphorescence from multiresponsive pure organic copolymers. *Ind. Eng. Chem. Res.* **59**, 1578–1583 (2020).
116. Hu, Y. Y., Dai, X. Y., Dong, X., Huo, M. & Liu, Y. Generation of tunable ultrastrong white-light emission by activation of a solid supramolecule through bromonaphthylpyridinium polymerization. *Angew. Chem. Int. Ed. Engl.* **61**, e202213097 (2022).
117. Ma, L. & Ma, X. Recent advances in room-temperature phosphorescent materials by manipulating intermolecular interactions. *Sci. China Chem.* **66**, 304–314 (2022).
118. Huang, Q., Lin, Z. & Yan, D. Tuning organic room-temperature phosphorescence through the confinement effect of inorganic micro/nanostructures. *Small Struct.* **2**, 2100044 (2021).
119. Ye, W. et al. Confining isolated chromophores for highly efficient blue phosphorescence. *Nat. Mater.* **20**, 1539–1544 (2021).
120. Wang, C., Liu, Y. H. & Liu, Y. Near-infrared phosphorescent switch of diarylethene phenylpyridinium derivative and cucurbit[8]uril for cell imaging. *Small* **18**, e2201821 (2022).
121. Yu, H. J. et al. A tunable full-color lanthanide noncovalent polymer based on cucurbituril-mediated supramolecular dimerization. *Chem. Sci.* **13**, 8187–8192 (2022).
122. Ma, X. K., Zhou, X., Wu, J., Shen, F. F. & Liu, Y. Two-photon excited near-infrared phosphorescence based on secondary supramolecular confinement. *Adv. Sci.* **9**, e2201182 (2022).
123. Huo, M., Dai, X. Y. & Liu, Y. Uncommon supramolecular phosphorescence-capturing assembly based on cucurbit[8]uril-mediated molecular folding for near-infrared lysosome imaging. *Small* **18**, e2104514 (2022).
124. Huo, M., Dai, X. Y. & Liu, Y. Ultrahigh supramolecular cascaded room-temperature phosphorescence capturing system. *Angew. Chem. Int. Ed. Engl.* **60**, 27171–27177 (2021).  
**This study describes a cascaded phosphorescence-capturing system in aqueous medium using cucurbit[7]uril and sulfonatocalix[4]arene.**
125. Huo, M., Dai, X. Y. & Liu, Y. Ultralarge Stokes shift phosphorescence artificial harvesting supramolecular system with near-infrared emission. *Adv. Sci.* **9**, e2201523 (2022).
126. Dai, X. Y. et al. A highly efficient phosphorescence/fluorescence supramolecular switch based on a bromoisquinoline cascaded assembly in aqueous solution. *Adv. Sci.* **9**, e2200524 (2022).
127. Wang, C. et al. Highly reversible supramolecular light switch for NIR phosphorescence resonance energy transfer. *Adv. Sci.* **9**, e2103041 (2022).
128. Wang, H. J., Xing, W. W., Zhang, H. Y., Xu, W. W. & Liu, Y. Cucurbit[8]uril confined 6-bromoisquinoline derivative dicationic phosphorescence energy transfer supramolecular switch for lysosome targeted imaging. *Adv. Opt. Mater.* **10**, 2201178 (2022).
129. Dang, Q. et al. Room-temperature phosphorescence resonance energy transfer for construction of near-infrared afterglow imaging agents. *Adv. Mater.* **32**, e2006752 (2020).
130. Liu, Z., Lin, W. & Liu, Y. Macrocyclic supramolecular assemblies based on hyaluronic acid and their biological applications. *Acc. Chem. Res.* **55**, 3417–3429 (2022).

131. Shen, F. F. et al. Purely organic light-harvesting phosphorescence energy transfer by  $\beta$ -cyclodextrin pseudorotaxane for mitochondria targeted imaging. *Chem. Sci.* **12**, 1851–1857 (2020).
132. Dai, X. Y., Huo, M., Dong, X., Hu, Y. Y. & Liu, Y. Noncovalent polymerization-activated ultrastrong near-infrared room-temperature phosphorescence energy transfer assembly in aqueous solution. *Adv. Mater.* **34**, e2203534 (2022).  
**This work reports the noncovalent polymerization-activated near-infrared phosphorescence-harvesting system in aqueous solution for targeted tumour cell imaging.**
133. Liu, Y. H. & Liu, Y. Highly efficient discrimination of cancer cells based on in situ-activated phosphorescence energy transfer for targeted cell imaging. *J. Mater. Chem. B* **10**, 8058–8063 (2022).
134. Zhou, W. L. et al. Multivalent supramolecular assembly with ultralong organic room temperature phosphorescence, high transfer efficiency and ultrahigh antenna effect in water. *Chem. Sci.* **13**, 573–579 (2022).
135. Shi, H., Wu, Y., Xu, J., Shi, H. & An, Z. Recent advances of carbon dots with afterglow emission. *Small* **19**, 2207104 (2023).
136. Teng, X., Sun, X., Pan, W., Song, Z. & Wang, J. Carbon dots confined in silica nanoparticles for triplet-to-singlet Förster resonance energy-transfer-induced delayed fluorescence. *ACS Appl. Nano Mater.* **5**, 5168–5175 (2022).
137. Liang, Y. C. et al. Phosphorescent carbon-nanodots-assisted Förster resonant energy transfer for achieving red afterglow in an aqueous solution. *ACS Nano* **15**, 16242–16254 (2021).
138. Mo, L. et al. Cascade resonance energy transfer for the construction of nanoparticles with multicolor long afterglow in aqueous solutions for information encryption and bioimaging. *Adv. Opt. Mater.* **10**, 2102666 (2022).
139. Li, T. et al. Phosphorescent carbon dots as long-lived donors to develop an energy transfer-based sensing platform. *Anal. Chem.* **95**, 2445–2451 (2023).
140. Voorhaar, L. & Hoogenboom, R. Supramolecular polymer networks: hydrogels and bulk materials. *Chem. Soc. Rev.* **45**, 4013–4031 (2016).
141. Lu, W., Le, X., Zhang, J., Huang, Y. & Chen, T. Supramolecular shape memory hydrogels: a new bridge between stimuli-responsive polymers and supramolecular chemistry. *Chem. Soc. Rev.* **46**, 1284–1294 (2017).
142. Chen, H., Ma, X., Wu, S. & Tian, H. A rapidly self-healing supramolecular polymer hydrogel with photostimulated room-temperature phosphorescence responsiveness. *Angew. Chem. Int. Ed. Engl.* **53**, 14149–14152 (2014).
143. Yuan, J. et al. Tunable dual emission of fluorescence-phosphorescence at room temperature based on pure organic supramolecular gels. *Dye. Pigment.* **181**, 108506 (2020).
144. Wang, H., Wang, H., Yang, X., Wang, Q. & Yang, Y. Ion-unquenchable and thermally “on-off” reversible room temperature phosphorescence of 3-bromoquinoline induced by supramolecular gels. *Langmuir* **31**, 486–491 (2015).
145. Chen, H., Xu, L., Ma, X. & Tian, H. Room temperature phosphorescence of 4-bromo-1,8-naphthalic anhydride derivative-based polyacrylamide copolymer with photo-stimulated responsiveness. *Polym. Chem.* **7**, 3989–3992 (2016).
146. Sun, X. R. et al. Supramolecular room-temperature phosphorescent hydrogel based on hexamethyl cucurbit[5]uril for cell imaging. *ACS Appl. Mater. Interfaces* **15**, 4668–4676 (2023).
147. Wei, L. et al. Triplet-triplet annihilation upconversion in LAPONITE®/PVP nanocomposites: absolute quantum yields of up to 23.8% in the solid state and application to anti-counterfeiting. *Mater. Horiz.* **9**, 3048–3056 (2022).
148. Kuila, S. et al. Aqueous phase phosphorescence: ambient triplet harvesting of purely organic phosphors via supramolecular scaffolding. *Angew. Chem. Int. Ed. Engl.* **57**, 17115–17119 (2018).
149. Garain, S., Garain, B. C., Eswaramoorthy, M., Pati, S. K. & George, S. J. Light-harvesting supramolecular phosphors: highly efficient room temperature phosphorescence in solution and hydrogels. *Angew. Chem. Int. Ed. Engl.* **60**, 19720–19724 (2021).  
**This work reports the high quantum yield solution-state phosphorescence which acts as light-harvesting scaffold to achieve delayed fluorescence in solution.**
150. Li, J. J., Zhang, H. Y., Zhang, Y., Zhou, W. L. & Liu, Y. Room-temperature phosphorescence and reversible white light switch based on a cyclodextrin polypseudorotaxane xerogel. *Adv. Opt. Mater.* **7**, 1900589 (2019).
151. Zhang, Y. et al. Photo-controlled reversible multicolor room-temperature phosphorescent solid supramolecular pseudopolyrotaxane. *Adv. Opt. Mater.* **10**, 2102169 (2022).
152. Zhou, Y. et al. Cucurbit[8]uril mediated ultralong purely organic phosphorescence and excellent mechanical strength performance in double-network supramolecular hydrogels. *Dye. Pigment.* **195**, 109725 (2021).
153. Zhang, T., Ma, X. & Tian, H. A facile way to obtain near-infrared room-temperature phosphorescent soft materials based on Bodipy dyes. *Chem. Sci.* **11**, 482–487 (2020).
154. Yu, J., Wang, H. & Liu, Y. Double-network confined supramolecular phosphorescence light-harvesting boosting photocatalysis. *Adv. Opt. Mater.* **10**, 2201761 (2022).
155. Hamzehpoor, E. et al. Efficient room-temperature phosphorescence of covalent organic frameworks through covalent halogen doping. *Nat. Chem.* **15**, 83–90 (2023).
156. Li, Y., Sui, J., Cui, L. S. & Jiang, H. L. Hydrogen bonding regulated flexibility and disorder in hydrazone-linked covalent organic frameworks. *J. Am. Chem. Soc.* **145**, 1359–1366 (2023).

## Acknowledgements

We thank National Natural Science Foundation of China (22131008) for the financial support.

## Author contributions

X.-Y.D. and M.H. contributed equally to this work. Y.L. revised the manuscript and conceived the overall orientation of the manuscript. All authors contributed to the discussion and editing of the manuscript before submission.

## Competing interest

The authors declare no competing interests.

## Additional information

**Supplementary information** The online version contains supplementary material available at <https://doi.org/10.1038/s41570-023-00555-1>.

**Peer review information** *Nature Reviews Chemistry* thanks the anonymous reviewers for their contribution to the peer review of this work.

**Publisher's note** Springer Nature remains neutral with regard to jurisdictional claims in published maps and institutional affiliations.

Springer Nature or its licensor (e.g. a society or other partner) holds exclusive rights to this article under a publishing agreement with the author(s) or other rightsholder(s); author self-archiving of the accepted manuscript version of this article is solely governed by the terms of such publishing agreement and applicable law.

© Springer Nature Limited 2023